NASA TECHNICAL
MEMORANDUM

NASA TM X-53777

1968

NASA TM X-53777

ASTRODYNAMICS, GUIDANCE AND OPTIMIZATION
RESEARCH AT MSFC

RESEARCH ACHIEVEMENTS REVIEW

VOLUME III REPORT NO. 2

RESEARCH AND DEVELOPMENT OPERATIONS
GEORGE C. MARSHALL SPACE FLIGHT CENTER
MARSHALL SPACE FLIGHT CENTER, ALABAMA

GEORGE C. MARSHALL SPACE FLIGHT CENTER

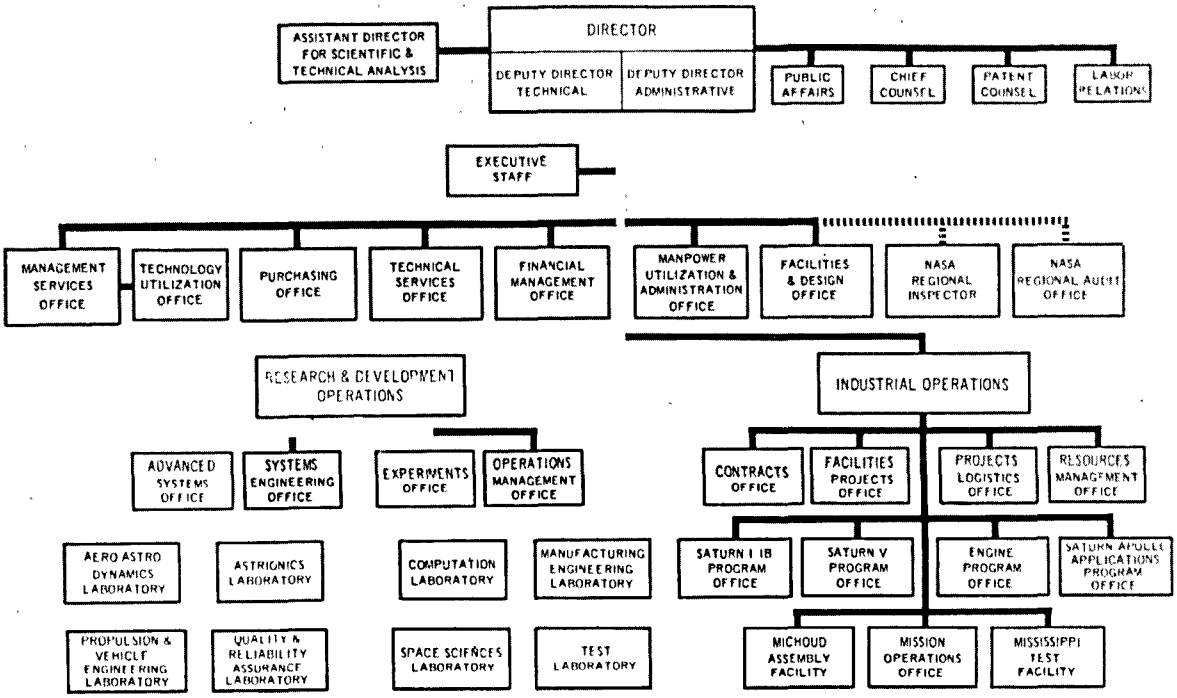

RESEARCH ACHIEVEMENTS REVIEWS COVER THE FOLLOWING FIELDS OF RESEARCH

- Radiation Physics
- Thermophysics
- Chemical Propulsion
- Cryogenic Technology
- Electronics
- Control Systems
- Materials
- Manufacturing
- Ground Testing
- Quality Assurance and Checkout
- Terrestrial and Space Environment
- Aerodynamics
- Instrumentation
- Power Systems
- Guidance Concepts
- Astrodynamics
- Advanced Tracking Systems
- Communication Systems
- Structures
- Mathematics and Computation
- Advanced Propulsion
- Lunar and Meteoroid Physics

NASA TM X-53777

NATIONAL AERONAUTICS AND SPACE ADMINISTRATION
WASHINGTON, D. C.

RESEARCH ACHIEVEMENTS REVIEW
VOLUME III REPORT NO. 2

ASTRODYNAMICS, GUIDANCE AND OPTIMIZATION RESEARCH AT MSFC

RESEARCH AND DEVELOPMENT OPERATIONS
GEORGE C. MARSHALL SPACE FLIGHT CENTER
MARSHALL SPACE FLIGHT CENTER, ALABAMA

1968

Page Intentionally Left Blank

PREFACE

In February, 1965, Dr. Ernst Stuhlinger, Director, Research Projects Laboratory (now Space Sciences Laboratory), initiated a series of Research Achievements Reviews which set forth those achievements accomplished by the laboratories of the Marshall Space Flight Center. Each review covered one or two fields of research in a form readily usable by specialists, systems engineers and program managers. The review of February 24, 1966, completed this series. Each review was documented in the "Research Achievements Review Series."

In March, 1966, a second series of Research Achievements Reviews was initiated. This second series emphasized research areas of greatest concentration of effort, of most rapid progress, or of most pertinent interest and was published as "Research Achievements Review Reports, Volume II." Volume II covered the reviews from March, 1966, through February, 1968.

This third series of Research Achievements Reviews was begun in March, 1968, and continues the concept introduced in the second series. Reviews of the third series are designated Volume III and will span the period from March, 1968, through February, 1970.

The papers in this report were presented May 22, 1968

William G. Johnson
Director
Experiments Office

Page Intentionally Left Blank

CONTENTS. . .

LIST OF ILLUSTRATIONS

LIST OF ILLUSTRATIONS

CONTENTS (Continued) . . .

LIST OF TABLES

LIST OF ILLUSTRATIONS

Page

OPTIMAL GUIDANCE

LIST OF ILLUSTRATIONS

Figure — Title

RENDEZVOUS TECHNIQUES

Page

LIST OF TABLES

LIST OF ILLUSTRATIONS

INTRODUCTION TO ASTRODYNAMICS, GUIDANCE AND OPTIMIZATION RESEARCH AT MSFC

By

Clyde D. Baker

The periodic Research Achievements Reviews afford an excellent opportunity for reporting to a wider audience some of the more significant results being generated by the Aero-Astrodynamics Laboratory. The concepts and ideas to be discussed in this review will be of particular interest and importance.

To express research results in an obscure manner as a detailed list of mathematical equations is the quickest and easiest approach. Unfortunately, such an approach conveys understanding to few people. The challenge then is to process and present the materials that evolve from the scientific studies being conducted in such a way that persons not directly connected with the area of research under discussion can easily grasp the concepts and ideas being presented and the achievements being accomplished. The papers which follow have to a large degree met this challenge successfully by reducing the abstract and obscure to a form that is both reasonable to read and easy to appreciate.

Three of the topics to be discussed bear a close relationship to each other. From an analytical point of view, the most general of the three is the paper by Lt. Schuyler Sampson on orbits in noncentral force fields. The discussion of the motion of an artificial satellite under the combined influence of planar and Keplerian force fields by Mr. Rowland Burns is a special case of the more general theory being examined by Lt. Sampson. While these two articles are entirely analytic, the third in this series, presented by Mr. J. Reynolds Duncan, Jr., represents the problem of generating interplanetary trajectories numerically by using interplanetary integrating computer programs.

The remaining two presentations are related to guidance. Mr. Hugo Ingram's paper presents a fairly broad class of guidance concepts with emphasis on optimization, while Mr. Wayne Deaton's paper deals specifically with the problems of rendezvous guidance techniques.

All of these papers succeed in expressing conceptually some of the difficult research tasks being undertaken by the Aero-Astrodynamics Laboratory, the direction being taken in the solution of the problems encountered in the studies, the accomplishments which are being achieved, and the goals which will be reached in the future.

Page Intentionally Left Blank

ORBITS IN NONCENTRAL FORCE FIELDS

By

Schuyler S. Sampson

LIST OF SYMBOLS

α = constant of integration

β = constant of integration

θ = angle between r and horizontal axis of coordinate system

ρ = semilatus recturn of a conic section

ϕ = constant angle

χ = transformed angular variable

a = constant

c = constant

D = region in space

e = eccentricity

E = constant total energy of system

F = force

h = 2 × angular momentum

H = Hamiltonian of a dynamical system

k = constant

l = constant

m = remote perturbing mass

M = central mass

p = momentum conjugate to coordinate appearing as subscript

r = distance from origin of coordinate system

$\vec{r}(t)$ = orbit determined by given initial conditions

S = function appearing in Hamilton-Jacobi equation

t = time

T = terminal time

V = potential energy in conservative force field

INTRODUCTION

It is frequently convenient in dealing with difficult problems in celestial mechanics to use an easily solved problem as an approximation to the actual situation. An example of this approach is a patched conic interplanetary trajectory. This author's research investigates a larger class of problems having closed form solutions that can be computed quickly.

DERIVATION OF EQUATIONS FOR NONCENTRAL ORBITS

Let a particle of unit mass move in a conservative field whose potential in polar coordinates is given by

$$V(r,\theta) = V_1(r) + V_2(\theta)/r^2 .$$

Then the Hamiltonian of the system is given by

$$H = \frac{1}{2}\left[p_r^2 + \frac{p_\theta^2}{r^2}\right] + V_1(r) + V_2(\theta)/r^2 = E$$

where E is the constant total energy.

The associated Hamilton-Jacobi equation is

$$\frac{1}{2}\left[\left(\frac{\partial S}{\partial r}\right)^2 + \frac{1}{r^2}\left(\frac{\partial S}{\partial \theta}\right)^2\right] + V_1(r) + \frac{V_2(\theta)}{r^2} = E$$

or

$$\frac{r^2}{2}\left(\frac{\partial S}{\partial r}\right)^2 + r^2 V_1(r) - r^2 E = -\frac{1}{2}\left(\frac{\partial S}{\partial \theta}\right)^2 - V_2(\theta) \tag{1}$$

Assume $S(r,\theta) = S_1(r) + S_2(\theta)$.

Then the left side of equation (1) is a function of r, and the right side is a function of θ. Setting each side of equation (1) equal to a constant, $-c^2$, gives

$$\frac{dS_1}{dr} = \left[2\left(E - V_1(r) - \frac{c^2}{r^2}\right)\right]^{\frac{1}{2}}$$

$$\frac{dS_2}{d\theta} = \left[2\left(c^2 - V_2(\theta)\right)\right]^{\frac{1}{2}}$$

$$S(r,\theta) = \int \left[2\left(E - V_1(r) - \frac{c^2}{r^2}\right)\right]^{\frac{1}{2}} dr + \int \left[2(e^2 - V_2(\theta)\right]^{\frac{1}{2}} d\theta$$

and the equations for the orbit are

$$\frac{\partial S}{\partial c^2} = (2)^{\frac{1}{2}}\left[\int \frac{-dr}{r^2\left(E - V_1(r) - \frac{c^2}{r^2}\right)^{\frac{1}{2}}} + \int \frac{d\theta}{\left(c^2 - V_2(\theta)\right)^{\frac{1}{2}}}\right] = \beta_1 \tag{2}$$

and

$$\frac{\partial S}{\partial E} = (2)^{\frac{1}{2}} \int \frac{dr}{\left(E - V_1(r) - \frac{c^2}{r^2}\right)^{\frac{1}{2}}} = \beta_2 + t \, . \tag{3}$$

Differentiating equations (2) and (3) with respect to r yields the more convenient relations

$$\dot{r} = \left[2\left(E - V_1(r) - \frac{c^2}{r^2}\right)\right]^{\frac{1}{2}} \tag{4}$$

and

$$\dot{\theta} = \left[2\left(c^2 - V_2(\theta)\right)\right]^{\frac{1}{2}} \, . \tag{5}$$

For initial experimentation it is convenient to restrict the forms of $V_1(r)$ and $V_2(\theta)$. Forms chosen are respectively

$$V_1(r) = -\frac{a}{r}$$

and

$$V_2(\theta) = -k \cos(\theta + \phi) - \ell \cos(\theta + \chi) - m \, .$$

Note that choosing $m \neq 0$ is equivalent to adding a term $-m/r^2$ to $V_1(r)$.

These selections give the equation of orbit shape

$$r = \frac{\rho}{1 - e\cos\left(\alpha + c\int \frac{d\theta}{\sqrt{c^2 - V_2(\theta)}}\right)} \, , \tag{6}$$

where $\rho = 2c^2/a^2$

$$e = [1 + 4c^2E/a^2]^{\frac{1}{2}} \, .$$

The orbit is bounded for $E < 0$, unbounded otherwise.

The constants of motion for these noncentral orbits are

E = total energy

and

$$c^2 = h^2/2 + V_2(\theta)$$

where h is twice the angular momentum.

From the form of equation (4) it is seen that these orbits are closely related to conic sections, qualitatively at least. In fact, if a non-uniformly rotating coordinate system is employed, then changing angular variables according to

$$\chi = c\int \frac{d\theta}{\left(c^2 - V_2(\theta)\right)^{\frac{1}{2}}}$$

yields

$$r = \frac{\rho}{1 - e \cos(\alpha + \chi)} .$$

EXAMPLES OF ORBITS

Consider a three-body system consisting of a "central" mass M, a "remote" perturbing mass m and an orbiting particle of unit mass, as shown in Figure 1. Then under the assumption that r does not vary too greatly, take

$$V_2(\theta) = -k \cos \theta$$

and a reasonably good approximation to the physical situation can be obtained. Figure 2 provides a comparison between the central orbit and the non-central orbit with the same initial conditions.

Figure 3 gives the same comparison in the case of an orbit that would be unbounded in the absence of a perturbing force.

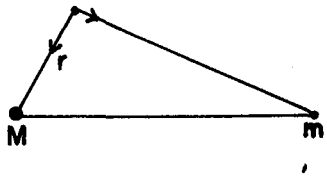

FIGURE 1. FORCE DIAGRAM

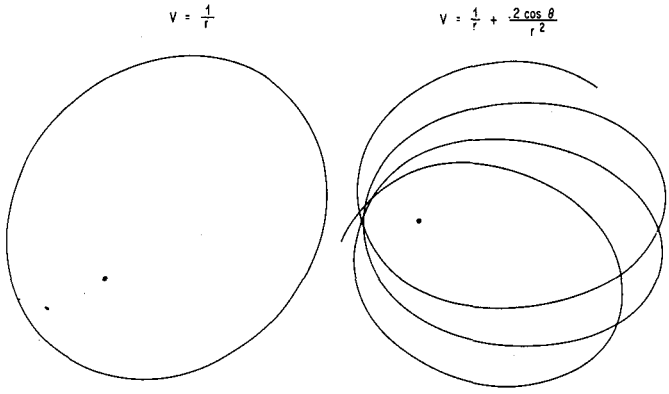

FIGURE 2. PERTURBED AND UNPERTURBED ORBITS (BOUNDED)

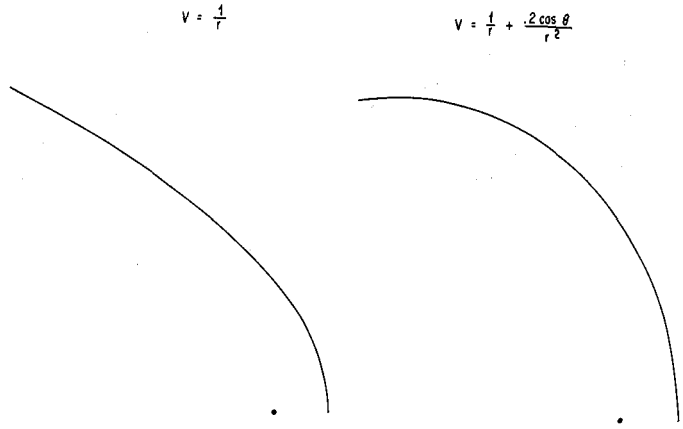

FIGURE 3. PERTURBED AND UNPERTURBED ORBITS (UNBOUNDED)

A COMPUTATIONAL PROBLEM

The equation

$$\dot{r} = \left[2\left(E - V_1(r) - \frac{c^2}{r^2}\right)\right]^{\frac{1}{2}}$$

is rather intractable from a computerized Runge-Kutta point of view, since $\dot{r}$ changes signs whenever r attains an extreme value. It is simpler and much more accurate to replace it by

$$\ddot{r} = \frac{2c^2}{r^3} - \frac{d\,V_1(r)}{d\,r} ,$$

which was used in plotting Figures 2 and 3.

UTILIZATION OF RESULTS

The basic problem of computing $V_1(r)$ and $V_2(\theta)$ may be formulated as follows:

given as data

$V(r, \theta)$, the potential arising from a physical situation and

$\left.\begin{matrix} r(0) \\ \dot{r}(0) \\ \theta(0) \\ \dot{\theta}(0) \end{matrix}\right\}$ initial conditions,

find $V_1(r)$, $V_2(\theta)/r^2$ such that the solution of the equations of motion (4) and (5) minimize the error of position as a function of time. That is, if $T > 0$ $\vec{r}(t)$ is the orbit associated with the initial conditions listed above and $\vec{\rho}(t)$ is the orbit obtained by replacing $V(r,\theta)$ with $V_1(r) + V_2(\theta)/r^2$, it may be desired to minimize either

$$|\vec{r}(T) - \vec{\rho}(T)|$$

or perhaps

$$\int_0^T |\vec{r}(t) - \vec{\rho}(t)|^2 \, dt .$$

This problem, unfortunately, has no closed form solution unless $\vec{r}(t)$ does. Therefore other functionals are selected which can be minimized conveniently. The two prime candidates for experimentation are

$$\iint_D \left[V(r,\theta) - V_1(r) - \frac{V_2(\theta)}{r^2} \right]^2 r \, dr \, d\theta \qquad (7)$$

and

$$\iint_D |F(r,\theta) - F^1(r,\theta)|^2 \, r \, dr \, d\theta , \qquad (8)$$

where D is a region in space

$$F(r,\theta) = \nabla V(r,\theta)$$

and

$$F^1(r,\theta) = \nabla (V_1(r) + V_2(\theta)/r^2) ;$$

$$\nabla f(r,\theta) = \left(\frac{\partial f}{\partial r} , \frac{1}{r} \frac{\partial f}{\partial \theta} \right) .$$

These functionals can be minimized by standard variational techniques. The problem becomes particularly simple if D is chosen to be the region

$$r_1 \le r \le r_2 ; \quad \theta_1 \le \theta \le \theta_2 .$$

Note that since no derivatives of the unknown functions appear in equation (7), the Euler equations for $V_1(r)$ and $V_2(\theta)$ will not contain any derivatives, so $V_1(r)$ and $V_2(\theta)$ can be found by algebraic manipulations.

REMAINING PROBLEMS

There are two aspects to the use of approximations. The first is the selection of the approximating function. In this case, that means finding a function to minimize. Hopefully something as simple as equation (7) will give an approximation that yields low errors in $\vec{r}(t)$. The only verification is by comparison of numerical data.

The second consideration is the determination of a region D where the approximation is good to within prescribed tolerances. There is no difficulty in establishing the numerical difference between two potential functions, but a knowledge of the cumulative error in position is required. This is not so easily discovered.

In order, then, to use these noncentral orbits for the computation of something like an interplanetary orbit, the following things must be done: (1) find the best local approximation to the physical situation, and (2) find a set of regions $D_1, D_2, \ldots, D_n$ including all of the trajectory so that the use of a k-th approximating function in D_k will yield an orbit sufficiently close to the actual orbit.

If this program proves unfeasible, an alternative solution is to use a noncentral orbit as an osculating orbit and to apply the principle of Encke's method.

A large class of problems in celestial mechanics admit closed form solutions and include all central orbits as special cases. This paper has indicated problems which remain to be solved, and two possible ways of applying these noncentral orbits to realistic situations. The long term expectation is that the very simple equations of motion associated with these orbits will permit much quicker calculation of complicated orbits than is now possible.

The class of orbits under discussion in this paper was observed previously by John P. Vinti of the National Bureau of Standards, but apparently only a few applications have been investigated thus far.

A CLOSED FORM SOLUTION FOR THE MOTION OF A SATELLITE UNDER KEPLERIAN AND PLANAR FORCE FIELDS

By

Rowland E. Burns

The bulk of today's research work in astronautics is numerical computation. Data from these computations are applicable to almost any problem and can be tailor-made to the specific problem under consideration. However, these data tell little about the general character of the problem.

This discussion is concerned with an analytical solution to the problem of radiation pressure on a satellite. This problem attained some measure of importance when the first Echo satellite was launched, because radiation pressure over a long period of time will perturb the orbit of a satellite. An analytical technique will provide an approximate solution to the radiation pressure problem; the exact nature of the method used can be illustrated by Figure 1. In Figure 1 the earth or some other similar attracting body is shown by the dotted line. The darker line is an unperturbed orbit (an ordinary Keplerian orbit such as an ellipse or circle). A parallel force field acting in the positive z direction is superimposed over these orbits to approximate the radiation pressure upon a satellite. In forcing the field to be completely parallel at all points, divergence of the field was neglected. Thus the problem is to define the type motion the satellite will experience when a parallel force field affects an inverse square attracting field from this planet.

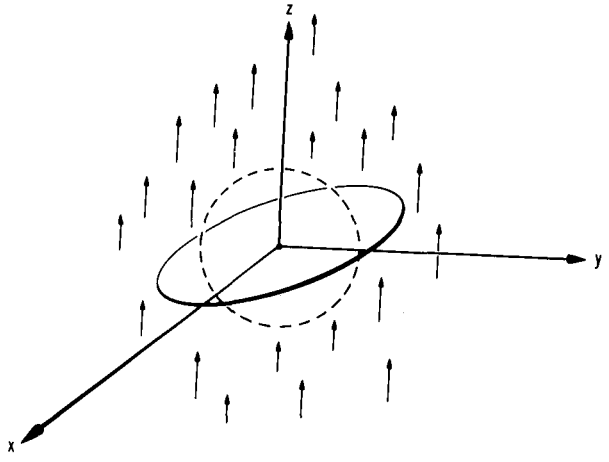

FIGURE 1. EARTH ORBIT (DOTTED LINE) AND KEPLERIAN ORBIT WITH PARALLEL FORCE FIELD IN Z DIRECTION

To the left in Figure 2 are the equations of ordinary Keplerian motion that were investigated by Newton several hundred years ago. The ordinary Keplerian orbits, such as circles, ellipses, hyperbolas, or parabolas, are obtained by integrating these three differential equations in which an inverse square force is proportional to the mass of the planet. To the right in Figure 2 appears to be a somewhat trival modification to these equations. The first two equations are identical to their counterparts on the left. The last equation has been modified by the addition of a constant. This constant now represents the planar force field that will perturb the Keplerian orbit. These are differential equations, and the addition of a constant of this sort can markedly change the results.

KEPLERIAN (INVERSE SQUARE FORCE) MOTION	PERTURBED (INVERSE SQUARE FORCE PLUS PLANAR FORCE) MOTION
$\ddot{x} = -\frac{\mu x}{(x^2 + y^2 + z^2)^{3/2}}$	$\ddot{x} = \frac{-\mu x}{(x^2 + y^2 + z^2)^{3/2}}$
$\ddot{y} = -\frac{\mu y}{(x^2 + y^2 + z^2)^{3/2}}$	$\ddot{y} = \frac{-\mu y}{(x^2 + y^2 + z^2)^{3/2}}$
$\ddot{z} = -\frac{\mu z}{(x^2 + y^2 + z^2)^{3/2}}$	$\ddot{z} = \frac{-\mu z}{(x^2 + y^2 + z^2)^{3/2}} + A$

FIGURE 2. SIMPLE AND MODIFIED KEPLERIAN EQUATIONS OF MOTION

To the left in Figure 3 is a system of spherical coordinates. To the right in Figure 3 is a rotational parabolic coordinate system that is useful in examining satellite orbits. Rather than having circles as lines of constant value of the coordinates, there are parabolas in some planes and circles in other planes (thus the rotational label). Use of this coordinate system is expedient and permits separation of equations.

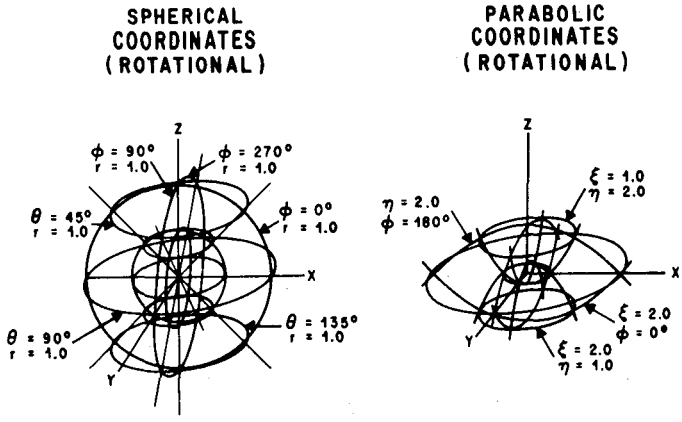

FIGURE 3. SPHERICAL AND PARABOLIC COORDINATES

In the top left part of Figure 4 are the differential equations of Keplerian motion for the two dimensional case. To the upper right are the equation of the orbit and the equation relating to the time (to the mean motion in the orbit). Below these equations on the left side, to illustrate the modification that occurs when a constant is added, are two equations (again for the two dimensional case). The first is the differential equation in x, and the second is a differential equation in z modified by the addition of a constant. To the right of these equations are the results of integrating these two equations. Comparison of the top equation of normal Keplerian motion with the top equation for perturbed Keplerian motion indicates the modification that occurs simply by addition of the constant A. The sn^{-1} is an inverse elliptic sine with some properties that parallel the ordinary inverse sine of circular trigonometry. The cn^{-1} is an inverse elliptic cosine. The first equation in the lower right hand block is the equation of the orbit if a constant, A, is added to the right side of the differential equation in z. It is a much more complicated equation than the Keplerian equation, because it describes the profusion of orbits that will be obtained. Below the equation of the perturbed orbit is an equation which relates the time in orbit to the position coordinates ξ and η. E is an ordinary elliptic integral. Just as the equation for the time is more complicated than the equation for the orbit in the Keplerian case, thus the bottom right hand equation for the time is more complicated than the equation for the orbit in the perturbed case.

KEPLERIAN

$$\ddot{x} = \frac{-\mu x}{(x^2+y^2+z^2)^{3/2}} \qquad r = \frac{a(1-e^2)}{1+e\cos\phi}$$

$$\ddot{z} = \frac{-\mu z}{(x^2+y^2+z^2)^{3/2}} \qquad t - t_0 = \frac{E - e\sin E}{n}$$

PERTURBED

$$\ddot{x} = \frac{-\mu x}{(x^2+y^2+z^2)^{3/2}}$$

$$\frac{1}{\sqrt{b_1}}\left[sn^{-1}\left(\sqrt{\frac{\xi}{a_1}}\cdot\sqrt{\frac{a_1}{b_1}}\right) - sn^{-1}\left(\sqrt{\frac{\xi_0}{a_1}}\cdot\sqrt{\frac{a_1}{b_1}}\right)\right] + \frac{1}{\sqrt{a_2+|b_2|}}\left[cn^{-1}\left(\sqrt{\frac{\eta_0}{a_2}}\cdot\sqrt{\frac{a_2}{a_2+|b_2|}}\right) - cn^{-1}\left(\sqrt{\frac{\eta}{a_2}}\cdot\sqrt{\frac{a_2}{a_2+|b_2|}}\right)\right]$$

$$\ddot{z} = \frac{-\mu z}{(x^2+y^2+z^2)^{3/2}} + A$$

$$t - t_0 = \sqrt{b_1}\left\{sn^{-1}\left(\sqrt{\frac{\zeta}{a_1}}\cdot\sqrt{\frac{a_1}{b_1}}\right) sn^{-1}\left(\sqrt{\frac{\xi_0}{a_1}}\cdot\sqrt{\frac{a_1}{b_1}}\right) - E\left[sn^{-1}\left(\sqrt{\frac{\xi}{a_1}}\cdot\sqrt{\frac{a_1}{b_1}}\right)\cdot\sqrt{\frac{a_1}{b_1}}\right] + E\left[sn^{-1}\left(\sqrt{\frac{\xi_0}{a_1}}\cdot\sqrt{\frac{a_1}{b_1}}\right)\cdot\sqrt{\frac{a_1}{b_1}}\right]\right\}$$

$$-\sqrt{a_2+|b_2|}\left\{E\left[cn^{-1}\left(\sqrt{\frac{\eta}{a_2}}\sqrt{\frac{a_2}{a_2+|b_2|}}\right)\cdot\sqrt{\frac{a_2}{a_2+|b_2|}}\right] - E\left[cn^{-1}\left(\sqrt{\frac{\eta_0}{a_2}}\cdot\sqrt{\frac{a_2}{a_2+|b_2|}}\right)\sqrt{\frac{a_2}{a_2+|b_2|}}\right]\right.$$

$$\left. - \frac{|b_2|}{a_2+|b_2|}\left[cn^{-1}\left(\sqrt{\frac{\eta}{a_2}}\cdot\sqrt{\frac{a_2}{a_2+|b_2|}}\right) - cn^{-1}\left(\sqrt{\frac{\eta}{a_2}}\cdot\sqrt{\frac{a_2}{a_2+|b_2|}}\right)\right]\right\}$$

FIGURE 4. POSITION AND TIME EQUATIONS FOR AN ORBIT

Figure 5 shows a circular orbit plotted in Cartesian coordinates. This has no planar force field superimposed upon it. Figure 5 and those to follow are two dimensional representations, because it is much more difficult to present three dimensional figures. In general, the values of A are chosen much higher than the values of A that occur for true radiation pressure problems. For very small values of A the resulting figures would be quite uninteresting; therefore the superimposed planar force field was given a much higher value than what is obtained in practice. Figure 5 and the following figures were machine plotted and may appear a little rough. Figure 5 is an unperturbed Keplerian orbit. Figure 6 is the same circle plotted in the parabolic coordinate system. The representation of the circle (Fig. 5) in parabolic coordinates (Fig. 6.) illustrates the results obtained by using the Cartesian coordinate system versus the parabolic coordinate system, respectively.

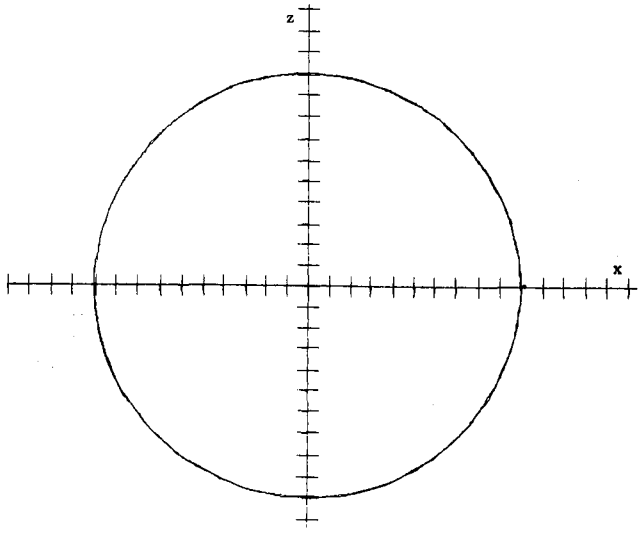

FIGURE 5. CIRCULAR ORBIT IN CARTESIAN COORDINATES, $Z_0 = \pm 1$, $A = 0$

A representation of a differential equation in z with a value of A = 0.001 is shown in Figure 7. A may be considered as a ratio of the initial planar force field to the gravitational force. In this case approximately 1/10 of 1% of the gravitational force is acting in the z direction. Figure 7 was plotted only to an arbitrary point in the orbit because of machine-time restrictions. For smaller values of A, which are more realistic, the orbit would almost

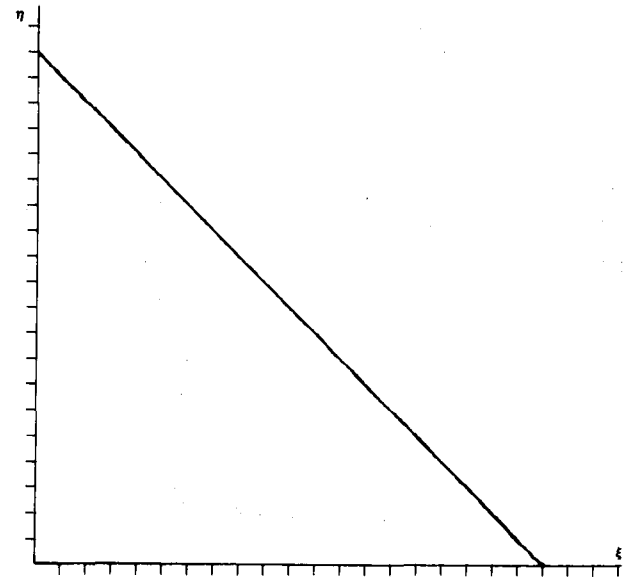

FIGURE 6. CIRCULAR ORBIT IN PARABOLIC COORDINATES, $Z_0 = \pm 1$, $A = 0$

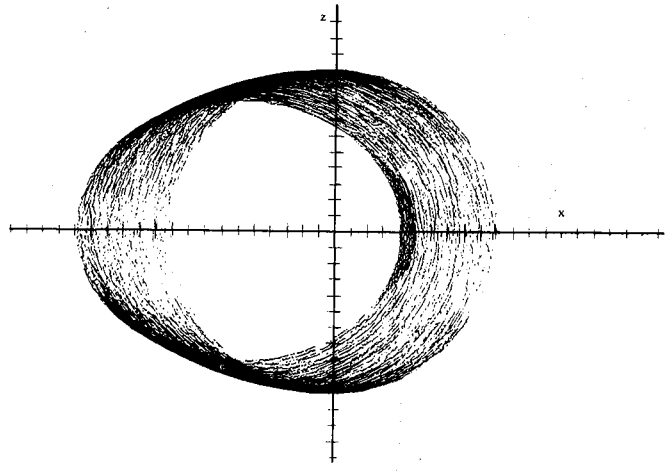

FIGURE 7. ORBIT IN CARTESIAN COORDINATES, $Z_0 = 1$, $A = 0.001$

retrace a constant path. Figure 7 is plotted in Cartesian coordinates. Figure 8 is the same orbit (A = 0.001) in parabolic coordinates. The equation shown in Figure 4 is an analytic representation of the orbit shown in Figure 8.

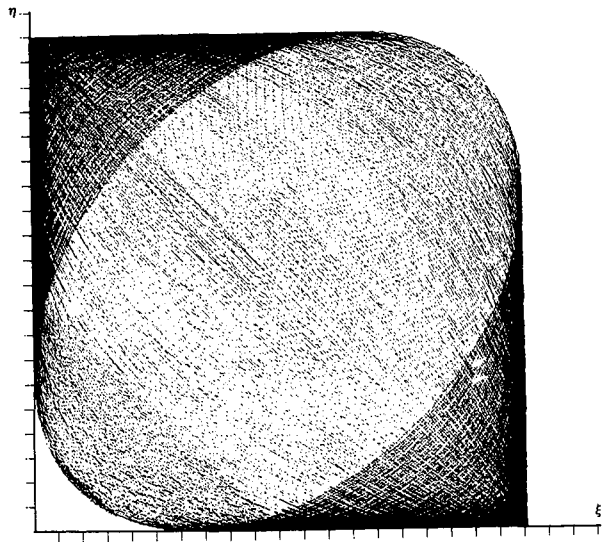

FIGURE 8. ORBIT IN PARABOLIC COORDINATES, $\dot{Z}_0 = 1$, A = 0.001

Figure 9 shows a value of the radiation pressure field of approximately 1% of the force of gravity. Some striking differences from Keplerian motion are beginning to appear. The satellite is initially in a circular orbit, and then is pushed to the right because the satellite in reality displays many of the aspects of gyroscopes. Finally, it is seen that all the orbits pass through a point in the right side of Figure 9. This point is slightly above the axis, thus indicating a force in that direction.

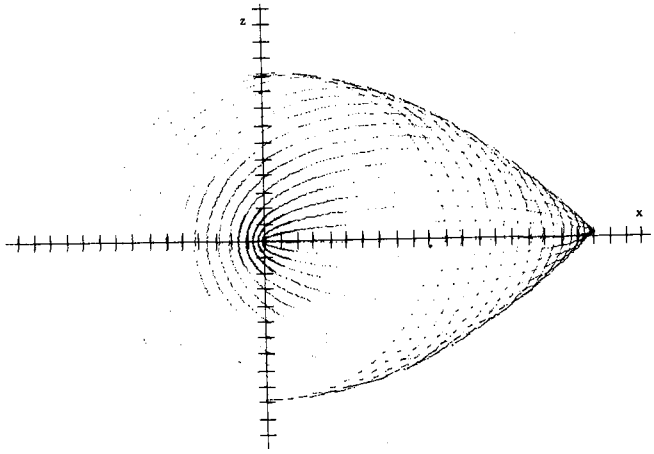

FIGURE 9. ORBIT IN CARTESIAN COORDINATES, $\dot{Z}_0 = -1$, A = 0.01

Figure 10 is the orbit in parabolic coordinates of the differential equation plotted in Figure 9. It now becomes apparent that parabolic coordinates are actually more applicable to the problem. In Figure 10 the satellite traces its path within the linear bounds on all four sides.

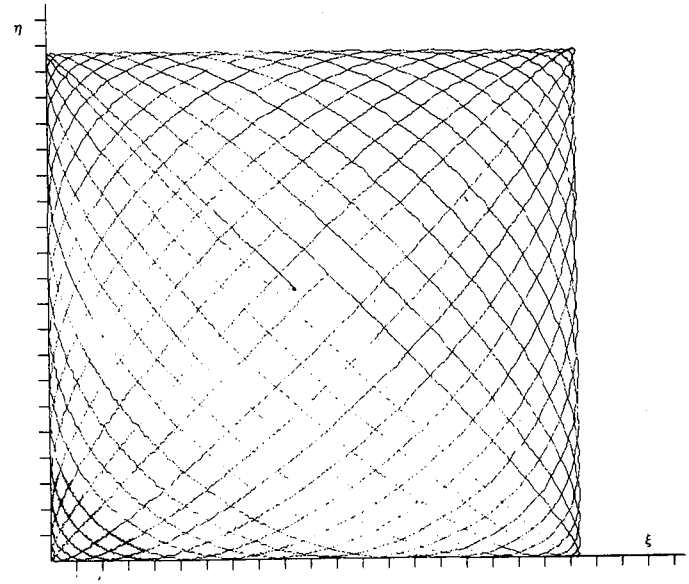

FIGURE 10. ORBIT IN PARABOLIC COORDINATES, $\dot{Z}_0 = -1$, A = 0.01

Increasing the radiation pressure further produces the extremely strange effects shown in Figure 11. At one point the orbit almost exhibits a cusp behavior. The radiation pressure has a value of 8% of the force of the gravitational field.

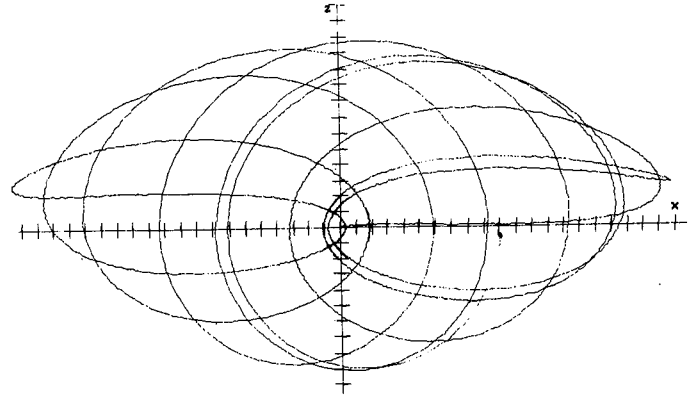

FIGURE 11. ORBIT IN CARTESIAN COORDINATES, $\dot{Z}_0 = -1$, A = 0.08

Figure 12 shows how necessarily complicated the equations of the orbit must be to represent all the various possible trajectories.

Figures 7 - 12 indicate how a minor modification of a differential equation can produce some profound changes in the physical results. The discussion has been limited to radiation pressure perturbations, but this may also apply to the type of orbit that could be achieved by a two body system with a very distantly removed gravitational attracting mass. At a very far distance the gravitational attraction will be essentially parallel as is the radiation pressure, though opposite in direction. This treatment also neglects such things as the motion of an earth satellite about the sun where the centrifugal accelerations caused by the motion of the earth in orbit become apparent.

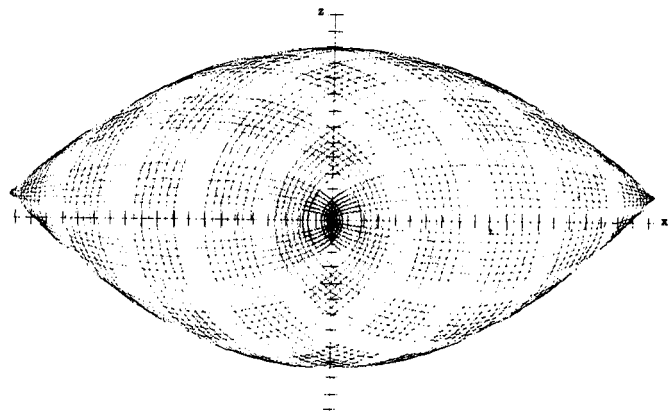

FIGURE 12. ORBIT IN CARTESIAN COORDINATES, $\dot{Z}_0 = -1$, $A = 0.05$

Page Intentionally Left Blank

A CRITICAL EVALUATION OF INTERPLANETARY INTEGRATING COMPUTER PROGRAMS

By

J. Reynolds Duncan, Jr.

This paper will discuss the initial phases of a long range research project concerning the critical evaluation of the components of interplanetary integrating computer programs. These evaluations should result in a meaningful classification of the advantages and disadvantages of not only the individual components but various combinations of these components. It is anticipated that the classifications will be made on the basis of such characteristics as speed, error control, versatility, and amenability to change.

A simple breakdown that indicates the basic structure of interplanetary integrating computer programs is shown on the left side of Figure 1. The arrows connecting these blocks with the block on the right side of Figure 1 indicate the dependence of the selection of the components of interplanetary programs upon the program goals or intended uses of the program. The first block on the left, N-body problem formulations, refers to the formulations of the equations of motion of a spacecraft subject to the spherically symmetric gravitational forces of massive bodies. Implied in this formulation is knowledge of the positions and velocities of the N-1 gravitating bodies that affect the motion of the spacecraft.

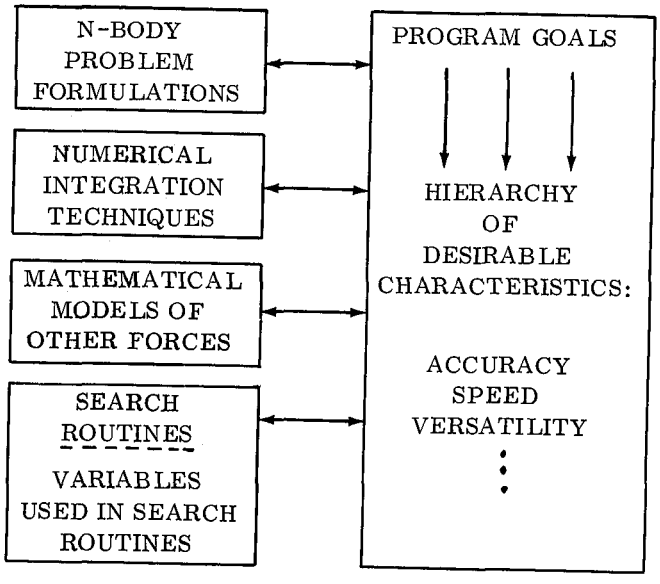

FIGURE 1. INTERPLANETARY INTEGRATING COMPUTER PROGRAMS

In the second block, or second part of the make-up of an interplanetary program, is indicated the techniques that are used to numerically integrate these equations of motion. The third part, mathematical models of other forces, refers to forces other than the spherically symmetric gravitational forces that are taken care of in the first block. These first three blocks form a trajectory generator or numerical integration program which, given a set of initial conditions and a time for the numerical integration to take place, will produce a set of final conditions. But these end conditions may not necessarily be the desired end conditions. Therefore, it is necessary to employ the use of a search routine or isolation routine whose purpose is to search for a set of initial conditions that will provide the desired set of terminal conditions, such as injection into a specific orbit about a distant planet. The dashed line indicates that the variables used in the search routine (the independent, dependent variables) may have some effect upon the operation of the search routine.

On the right side of Figure 1 are the program goals that can be expanded into a hierarchy of desirable characteristics. These characteristics are the properties the program should have in order to obtain the desired goals. Actually the construction of this list of desirable characteristics is not as simple as just indicating which things are to be desired in the program because many, if not all, of these characteristics are of a competing nature. For example, if you wish to have a program that is very accurate, then you will probably need to increase the running time of the program to attain this higher accuracy, thus improving one program characteristic at the expense of another. So, instead of an ordered list, it would be better to assign weighted values to each of the characteristics and thus indicate not only their relative importance, but how much you might

be willing to trade off one characteristic against another in order to achieve a program with the best combination of desired properties.

Now that an outline has been given of the overall structure of interplanetary programs, each one of the blocks in Figure 1 will be discussed individually in more detail to develop a better understanding of the components that are under study. Three principal formulations for the equations of motion of spacecraft are listed in Table I. It is one of these three formulations, or a combination or variation of these formulations, that is used in almost all of the interplanetary computer programs. The first one, direct summation of forces, is the simplest most straightforward method of formulating the equations of motion. It is often referred to as a Cowell formulation. The second and third formulations make use of reference orbits. When two-body motion is used for the reference orbit in the variation of coordinates method, the formulation is usually referred to as an Encke formulation. It is not necessary to use two-body motion for the reference orbit, since the only requirement is that the reference orbit that is used should have a closed form solution. As is indicated by the name, variation of coordinates, the only variables that are actually numerically integrated in this formulation are the variations from a reference orbit. The third formulation, variation of parameters, is very similar to the second in some ways. The orbit itself, instead of being represented in Cartesian coordinates, is represented in terms of orbital elements or parameters. It is the variation of these orbital elements or parameters from the reference orbit which is actually numerically integrated.

TABLE I. PRINCIPAL FORMULATIONS

• DIRECT SUMMATION OF FORCES
• VARIATION OF COORDINATES
• VARIATION OF PARAMETERS

Next, some of the numerical integration techniques used will be examined. Table II is a list of some of the many integration techniques in use today. This paper will not describe the detailed structure of each one of these techniques, but a great number and variety of techniques exist. Some of these techniques lend themselves well to numerical integration with small fixed time steps over relatively short periods of time, while others have the advantage of using variable time steps and may be used for numerical integration in interplanetary space where it is advantageous to use a variable Δt. Some of the routines do not have error control built into them and do not offer any indication of how accurately the numerical integration is being performed, whereas other techniques lend themselves well to error control or provide an indication of the numerical errors that are accumulating in the numerical integration process.

TABLE II. NUMERICAL INTEGRATION TECHNIQUES

• ADAMS-MOULTON
• RUNGE-KUTTA
• SHANKS
• FEHLBERG
• POWER SERIES

Table III lists some of the additional mathematical models that may need to be included in an interplanetary program, depending upon the desired accuracy of the program. The nonspherical gravitational forces refer to those forces that arise from the nonspherically symmetric nature of those gravitational bodies that affect the path of the spacecraft. The aerodynamic forces, of course, refer to the atmospheric drag that may be encountered by a spacecraft. The propulsive forces, which may require inclusion, are both of an intentional and unintentional nature: the intentional part is the nominal thrusting of a rocket motor for a boost into orbit or a midcourse maneuver; the unintentional part is the off-nominal performance of the rocket motor and such things as out-gassing and leaky valves aboard a spacecraft. Solar radiation pressure is the force caused by the impact of photons striking a spacecraft. Although this effect may be small, it is cumulative, and can noticeably perturb the path of an interplanetary spacecraft. Electromagnetic forces can affect the orbit of a spacecraft traveling through ionized gasses. The bombardment of a spacecraft by the heavier particle emission from the sun (the solar wind) can also cause noticeable perturbations from a desired path. Depending upon the desired accuracy of the program, relativistic effects, as well as other forces not listed here, may need to be mathematically modeled and included in an interplanetary program.

Table IV lists a few of the search routines that are currently being used. These and the other routines not listed have basic similarities; most of them use partial derivatives, some use first order partials,

TABLE III. MATHEMATICAL MODELS

• NON-SHPERICAL GRAVITATIONAL FORCES
• AERODYNAMIC FORCES
• PROPULSIVE FORCES
• SOLAR RADIATION PRESSURE
• ELECTROMAGNETIC FORCES
• SOLAR WIND
• RELATIVITY EFFECTS

others use second order and higher partial derivatives. Even with these similarities there is a wide range of performance with some routines having rapid convergence over a small area and other routines having much slower convergence over a considerably larger area. Therefore, with regard to search routines, the objectives of this investigation are to identify all the advantages and disadvantages of each of these routines and indicate how well or efficiently they operate with other parts of the program.

TABLE IV. SEARCH ROUTINES

• SECANT METHOD
• NEWTON'S METHOD BY DIVIDED DIFFERENCES
• STEEPEST DESCENT
• NEWTON'S METHOD WITH INTEGRATED PARTIAL DERIVATIVES
• GENERALIZED NEWTON-RHAPSON

To indicate how the results of this study may be of use, two sample interplanetary programs are shown in Figures 2 and 3. These hypothetical programs were constructed based upon preliminary

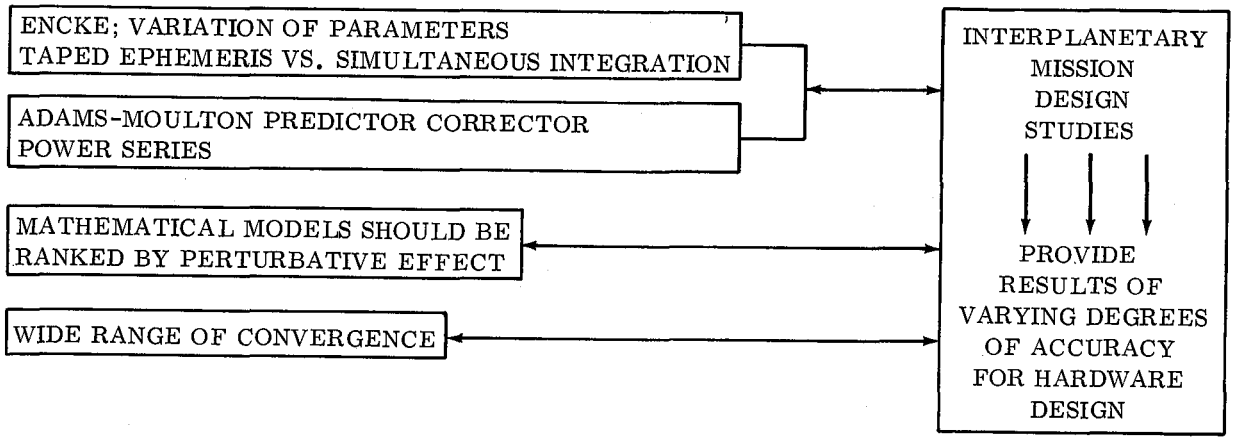

FIGURE 2. INTERPLANETARY NUMERICALLY INTEGRATING PROGRAM FOR MISSION DESIGN STUDIES

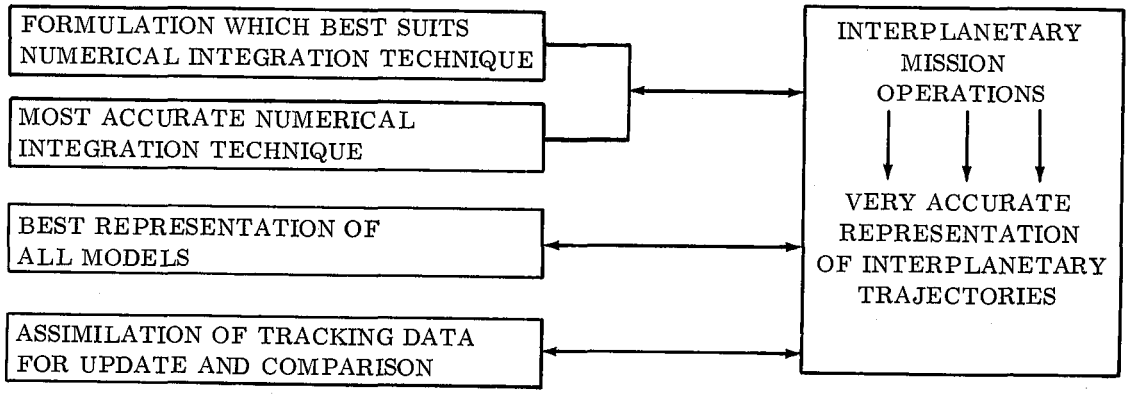

FIGURE 3. INTERPLANETARY TRAJECTORY PROGRAM FOR MISSION OPERATIONS

investigations and are presented only as examples of how the projected study results may be used. The format for the breakdown of the programs is the same as that used in Figure 1.

In Figure 2 is shown an interplanetary numerically integrating program that is intended for use primarily in mission design studies. A possible desirable characteristic or trait of this type of program would be to provide results of varying degrees of accuracy for hardware design. These results of varying accuracy are suggested by the nature of design studies. In the initial phases of many mission design studies, the input parameters that are needed for the computation of design trajectories are often not well known and may be little more than guesses or best estimates. Also, in the initial phases, the number of trajectories that are used in the design of the hardware for an interplanetary spacecraft may be quite large compared to the number that would be needed in later phases when more accurate values of the input parameters are known. If a program could provide results commensurate with the accuracy of the input parameters, this may result in a considerable savings in computer running time.

In the blocks on the left side on Figure 2 are indicated some choices or characteristics of the components that might be used in the construction of this type of a program. The line joining the first two blocks indicates that the evaluation of the combination of the numerical integration technique with the formulation of the equations of motion may be more important than the separate evaluation of these components. That is, since these two components work very closely together, a better measure of their efficiency might be to evaluate them together rather than separately. Indicated in the first block is the use of Encke or variation of parameters in the formulation of the equations of motion. These were chosen since most of the interplanetary trajectories will be numerically integrated in heliocentric space for which these formulations are well adapted. Also indicated is another possible choice, and that is the use of a taped ephemeris versus simultaneous integration. In most N-body problem simulations, where all the planets are represented, use is quite often made of a taped ephemeris where the positions and velocity of the planets for a future time span (20 or 30 years) are precomputed and stored on tape. Then, the values needed for the numerical integration of a trajectory are retrieved and interpolated. If the required accuracy of the program is not precise, and it would not be in the initial phases of a mission design study, it may be possible to use a two or three massive body simulation. Then the equations of motion of the massive bodies, such as the sun, the earth, and the target planet may be simultaneously integrated with the equations of motion of the spacecraft. It is possible that this method may provide some saving in computer running time. In the second block are indicated two possible choices for a numerical integration technique. The Adams-Moulton predictor-corrector technique is probably one of the techniques most widely used in interplanetary programs. Another possibility is the use of power series for the numerical integration procedure. Both of these techniques are well suited for this type of numerical integration. Whatever technique is used should be capable of integrating with an easily controlled variable degree of accuracy to satisfy the requirement of a variable accuracy trajectory.

In block number three it is indicated that the mathematical models should be ranked by perturbative effect. This would be very helpful in constructing the type of program indicated in Figure 2. It would then be possible to include or exclude those models needed to maintain but not exceed a specified degree of accuracy. Of course, the fewer models used, the faster the program operations can proceed. Then, as the desired accuracy increases, additional models could be added with the most perturbing forces being added first and the least perturbing forces added later, if needed. One of the goals of this study is to attempt to rank these models in this fashion so that they will be available for use in such programs.

As indicated in the fourth block, one advantageous property of a search routine for this type of program would be a wide-range convergence of the search routine, since, as previously mentioned, some of the initial trajectories that would be run would probably be based upon guesses or best estimates of the input parameters.

Shown in Figure 3 is another example of an interplanetary trajectory program, but this one has a quite different function. Its main purpose would be for use in mission operations, which, in this sense, would be the interplanetary program used to numerically determine the path of a spacecraft after launch. The program would therefore be used in the determination of such things as the time of firing of the midcourse engines, the time of firing of the engine to inject the spacecraft into orbit about another planet, and may be used in the selection of the proper time for activating a camera or videcon for taking television pictures or photographs about

another planet. To perform these and other tasks, it is important that the program give very accurate representations of interplanetary trajectories. With this as a desirable characteristic, certain requirements can be placed upon the components of such a program. As in Figure 2, the line joining the first two blocks indicates that consideration of the union of these blocks is probably more important than their separate consideration. As indicated within the blocks, the selection of the formulation should be based upon which formulation best suits the numerical integration technique. Since accuracy is of prime importance, the numerical integration technique chosen should, of course, be the most accurate technique available. The models used (block 3) should be the best representations that are available. As indicated in block 3, all of the models should be used so that the resulting trajectory will correspond as closely as possible to the actual interplanetary trajectory. In this interplanetary mission operations program, use would not necessarily have to be made of an isolation or search routine, but the program itself would have to have the capability of assimilating tracking data for updating and comparison purposes. (see block 4.) With the addition of this particular function, the program might more accurately be called an orbit determination program.

By use of these two sample programs, an attempt has been made to illustrate the impact of the intended use of the program upon the construction of interplanetary programs and to explain the value of having available a detailed analysis of the properties of the various components and combinations of these components. The study has not yet reached the point where specific recommendations can be made concerning the construction of particular interplanetary programs; however, some of the basic formulations, in combination with different numerical integration techniques, are now being readied for computer checkout. Upon completion of the study, the results should not only be applicable for the construction of efficient programs with a resultant reduction of computer running time, but also these results should provide some added degree of confidence to the user of the interplanetary programs which are presently available.

Page Intentionally Left Blank

OPTIMAL GUIDANCE

By

Hugo Ingram

The topics discussed in this paper are the mathematical formulation for optimal guidance and the effort involved in the implementation of optimal guidance. Also, this work is compared with the present iterative guidance mode (IGM) onboard guidance scheme. In order to fully understand an optimal guidance procedure, it is first necessary to understand how to compute an optimal trajectory; therefore, the first part of this paper will be a brief description of the optimal trajectory problem.

Figure 1 is a pictorial representation of the optimal trajectory problem. A set of functions to be satisfied at the initial time are to be connected by a trajectory to a set of functions that are to be satisfied at the final time. The trajectory connecting the initial functions, F, to the final functions, G, is determined by a set of ordinary first order differential equations (the $\dot{x}$'s) usually referred to as the equations of motion. Vector notation is used in Figure 1 and thus x is a vector with components that denote the state of the trajectory at a particular instant. For example, in a rocket trajectory the state is characterized by the following quantities: x, y, and z (the position vector), $\dot{x}$, $\dot{y}$, and $\dot{z}$ (the velocity vector), and F/m_0 and $\dot{m}/m_0$ (the performance characteristics). The parameters α and β are parameters which can be specified arbitrarily at the initial and final times, and the parameters u are called the control variables which are also assumed to be able to be specified arbitrarily at any instant of time. Thus the determination of the optimal trajectory (denoted by the solid line in Figure 1) involves the selection of the parameters α, β, and u such that the quantity J is maximized or minimized. Usually the function J in Figure 1 is just the mass at the final time; the F's represent the initial state of the vehicle; the G's represent the desired end conditions (for example circular orbit conditions).

To minimize or maximize J subject to the constraints of the problem, it is necessary to define a new quantity J' as is shown in Figure 2. J' is equal to J when the constraints are satisfied [i.e., when F and G = 0 and $x = F(x, u)$]. At this point it will be advantageous to note that discontinuities in the state

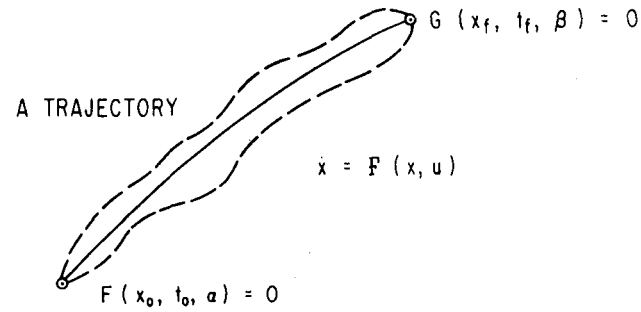

TO BE OPTIMIZED

$$J = \Phi(x_0, t_0) + \psi(x_f, t_f) + \int_{t_0}^{t_f} f(x, u)\, dt$$

FIGURE 1. THE MATHEMATICAL SIMULATION OF A TRAJECTORY

variables can occur at points between t_0 and t_f. If these discontinuities occur at times such as t_1 and t_2, then the integral in J and J' can be divided into parts as follows

$$\int_{t_0}^{t_1} + \int_{t_1}^{t_2} + \int_{t_2}^{t_f} .$$

Also, the specified discontinuities at t_1 and t_2 can be considered as constraints and adjoined to J' with additional multipliers just as the functions F and G were adjoined with the multipliers p and ρ and the differential constraints $\dot{x} = F(x, u)$ with the λ's. For simplicity this is not done in Figure 2 and J' is written only for a one stage problem, but the additional work for multiple stages is not difficult conceptually and has been performed for staging discontinuities and for coast-arc discontinuities.

The first variation for J' is also given in Figure 2. This must be zero in order for J' to be a maximum or a minimum. The second variation, which is not written out, must then be examined to determine whether J' is maximized or minimized when $\Delta J' = 0$. Then in Figure 3 the conditions necessary for causing $\Delta J'$ to be zero are given. When taken all together,

$$J' = \Phi(x_0, t_0) + P^T F(x_0, t_0, \alpha) + \psi(x_f, t_f) + \rho^T G(x_f, t_f, \beta) + \int_{t_0}^{t_f} \left\{ f(x, u) + \lambda^T \left[\dot{x} - F(x, u) \right] \right\} dt$$

$$\begin{aligned} \Delta J' = {} & \Phi_{x_0} \Delta x_0 + (\Phi_{x_0} \dot{x}_0 + \Phi_{t_0}) \Delta t_0 + \Delta P^T F_0 \\ & + P^T \left[F_{x_0} \Delta x_0 + (F_{x_0} \dot{x}_0 + F_{t_0}) \Delta t_0 + F_\alpha \Delta \alpha \right] \\ & + \psi_{x_f} \Delta x_f + (\psi_{x_f} \dot{x}_f + \psi_{t_f}) \Delta t_f + \Delta \rho^T G_f \\ & + \rho^T \left[G_{x_f} \Delta x_f + (G_{x_f} \dot{x}_f + F_{t_f}) \Delta t_f + G_\beta \Delta \beta \right] \\ & - \left\{ f(x_0, u_0) + \lambda_0^T \left[\dot{x}_0 - F_0 \right] \right\} \Delta t_0 + \left\{ f(x_f, u_0) + \lambda_f^T \left[\dot{x}_f - F_f \right] \right\} \\ & + \int_{t_0}^{t_0} \left[f_x \Delta x + f_u \Delta u + \Delta \lambda^T (\dot{x} - F) + \lambda^T (\Delta \dot{x} - F_x \Delta x - F_u \Delta u) \right] dt \end{aligned}$$

FIGURE 2. THE OPTIMIZATION TECHNIQUE

these conditions form the boundary value problem for the determination of an optimal trajectory. To solve this boundary value problem, initial guesses are selected for x_0, t_0, α, p, ρ, β, and t_f. With this information the initial constraints can be evaluated, the differential constraints integrated (usually numerically since the equations are nonlinear), and then the terminal constraints evaluated. Naturally, the initial constraints and the terminal constraints will not usually be satisfied for the guessed initial conditions, but there are many techniques available for using the amount that the initial and terminal conditions are not satisfied to compute corrections to the initial guesses. This procedure will more nearly satisfy the boundary value problem and thus finally yield an optimal trajectory. References 1 and 2 describe some of these procedures. This concludes the brief description of the techniques necessary for the determination of an optimal trajectory.

In Figure 4 the necessary conditions for the optimal guidance boundary value problem are given. It should be noticed immediately that this problem is almost identical to the optimal trajectory problem. The only difference is that the initial constraints are eliminated from the problem because when active guidance is used, the vehicle must determine its present state. These conditions are then fixed and the optimal guidance problem is to determine an optimal trajectory that connects these measured initial conditions with the desired terminal constraints. Thus the number of guessed initial conditions is reduced to only λ_0, t_f, ρ, and β as is shown in Figure 4. It is usually assumed at this point that it is too difficult to use this approach for actual onboard guidance, and thus many approximations are attempted to simplify the guidance boundary value problem so that is may be used in a form suitable for onboard computations. Some of these approaches will now be discussed and then some more details about

$$\text{INITIAL CONSTRAINTS} \begin{cases} F(x_0, t_0, \alpha) = 0 \\ \lambda_0^T = \Phi_{x_0} + P^T F_{x_0} \\ H_0 + \Phi_{t_0} + P^T F_{t_0} = 0 \\ P^T F_\alpha = 0 \end{cases}$$

H AT ANY TIME IS DEFINED AS $H = \lambda^T F(x, u) - f(x, u)$

$$\text{DIFFERENTIAL CONSTRAINTS} \begin{cases} \dot{x} = H_\lambda^T \\ \dot{\lambda} = -H_x^T \\ 0 = H_u \end{cases}$$

$$\text{TERMINAL CONSTRAINTS} \begin{cases} G(x_f, t_f, \beta) = 0 \\ \lambda_f^T = -\psi_{x_f} - \rho^T G_{x_f} \\ H_f - \psi_{t_f} - \rho^T G_{t_f} = 0 \\ \rho^T G_\beta = 0 \end{cases}$$

FIGURE 3. THE NECESSARY CONDITIONS

GIVEN x_0, t_0

DETERMINE FOR THE
GENERATION OF THE GUIDANCE SIGNAL, $\lambda_0, t_f, \rho, \beta$

SUBJECT TO:

DIFFERENTIAL CONSTRAINTS

$$\begin{cases} \dot{x} = H_\lambda^T \\ \dot{\lambda} = -H_x^T \\ 0 = H_u \end{cases}$$

TERMINAL CONSTRAINTS

$$\begin{cases} G(x_f, t_f, \beta) = 0 \\ \lambda_f^T = -\psi_{x_f} - \rho^T G_{x_f} \\ H_f - \psi_{t_f} - \rho^T G_{t_f} = 0 \\ \rho^T G\beta = 0 \end{cases}$$

FIGURE 4. THE GUIDANCE BOUNDARY VALUE PROBLEM

possible implementation of complete optimal guidance will be mentioned.

Figure 5 is an enumeration of the principal approximations that are made for the implementation of the present IGM guidance scheme. Approximations (1) and (2) allow the differential equations or the equations of motion to be solved in closed form. Then these closed form solutions can be substituted into the terminal constraints to yield a system of nonlinear equations which must be solved for A, B, and t_f. This can only be done in explicit form by making some more simplifying approximations which then yield the final form of the IGM guidance equations which are given in Reference 3. It must be noted that approximation (1) listed in Figure 5 eliminates any consideration of optimality and thus also eliminates the transversality conditions so that only the physical boundary conditions (the G's) must be satisfied as terminal constraints. It has been observed, however, that numerical simulations of the IGM guidance procedure perform extremely well in obtaining the desired terminal conditions and the deviations from an optimal trajectory are usually insignificant.

Figure 6 is an improvement of the IGM guidance procedure that is somewhat similar in approach. The principal approximation is the assumption of a constant gravity. Then the problem is formulated and solved as an optimal trajectory problem or as the guidance boundary value problem of Figure 4. Again the assumption of a constant gravity allows the differential constraints (both the $\dot{x}$'s and the $\dot{\lambda}$'s) to be integrated in closed form which results in a system of simultaneous nonlinear equations (the terminal constraints) which must be solved for the unknowns λ_0, t_f, ρ, and β. For this procedure no additional approximations are made to solve the system of nonlinear equations. Instead a numerical procedure such as Newton's method, Reference 1, or the Secant method, Reference 2, is used. Numerical simulations of this procedure have been performed and a paper on more details and improvements has been prepared for the AIAA Guidance, Control, and Flight Dynamics Conference to be held in Pasadena, California, in August 1968 [2].

A summary of the three guidance schemes discussed here is given in Figure 7. The first and most desirable scheme for implementation is called optimal guidance, which involves numerical integration of the differential constraints and a numerical solution of the boundary value simultaneous equations. The second approach is called quasi optimum trajectory analysis (QUOTA). The only difference in this approach is the simplifying assumption of a constant gravity which allows a closed form solution of the differential equations and eliminates the necessity of

(1.) $U = A + B\,t$

(2) CONSTANT GRAVITY (MAGNITUDE AND DIRECTION)

THEN THE BOUNDARY VALUE PROBLEM BECOMES;
DETERMINE A, B, AND t_f SUBJECT TO:

DIFFERENTIAL CONSTRAINTS

$$\dot{x} = F(x,u)$$

TERMINAL CONSTRAINTS

$$G(x_f, t_f) = 0$$

FIGURE 5. APPROXIMATIONS FOR IMPLEMENTATION OF IGM

(1.) CONSTANT GRAVITY (MAGNITUDE AND DIRECTION). THEN THE BOUNDARY VALUE PROBLEM BECOMES;

DETERMINE λ_0, t_f, ρ, AND β SUBJECT TO:

DIFFERENTIAL CONSTRAINTS

$$\dot{x} = H_\lambda^T$$
$$\dot{\lambda} = -H_x^T$$
$$0 = H_u$$

TERMINAL CONSTRAINTS

$$G(x_f, t_f, \beta) = 0$$
$$\lambda(t_f) = -\psi_{x_f} - \rho^T G_{x_f}$$
$$H_f - \psi_{t_f} - \rho^T G_{t_f} = 0$$
$$\rho^T G_\beta = 0$$

FIGURE 6. APPROXIMATIONS FOR IMPLEMENTATION OF QUOTA

I. OPTIMAL GUIDANCE

(A.) NUMERICAL INTEGRATION OF DIFFERENTIAL CONSTRAINTS

(B.) NUMERICAL SOLUTION OF BOUNDARY VALUE SIMULTANEOUS EQUATIONS

II. QUOTA

(A.) APPROXIMATION OF CONSTANT GRAVITY ALLOWS CLOSED FORM SOLUTION OF *ALL* THE DIFFERENTIAL CONSTRAINTS

(B.) NUMERICAL SOLUTION OF BOUNDARY VALUE SIMULTANEOUS EQUATIONS

III. IGM

(A.) APPROXIMATIONS OF A LINEAR X PROGRAM AND A CONSTANT GRAVITY NECESSITATES A CLOSED FORM SOLUTION OF *ONLY* THE EQUATIONS OF MOTION

(B.) AN ALMOST EXPLICIT SOLUTION FOR A, B, AND t_f IS OBTAINED USING *ONLY* THE PHYSICAL BOUNDARY CONDITIONS

FIGURE 7. COMPARISON OF GUIDANCE SCHEMES

numerical integration. The third approach is the present IGM guidance equations, which does not involve either the numerical integration or the numerical solution of the boundary value problem. This is the approach which is implemented for flight vehicles primarily due to the limitations of the present onboard guidance computer. It is hoped that future guidance computers will allow the more complicated but more effective procedures listed in Figure 7 to be used as onboard guidance schemes. Even if this is not the case, mathematical simulations of the first two procedures will still prove useful for comparison with the IGM procedure. For example, References 4 and 5 give some comparisons of Optimal Guidance and QUOTA with IGM.

Figure 8 indicates several approaches to improving the implementation of optimal guidance for onboard use. The first improvement listed is the preflight solution of the guidance boundary value problem for a nominal set of initial conditions. When these solution unknowns are used as initial guesses for the onboard solution of the optimal guidance problem, the work and time used for a particular guidance cycle is greatly decreased. The second preflight calculation that can be made is the determination of the matrix $[P_0]$, which tells how the nominal unknowns vary with respect to changes in the nominal initial state for the guidance boundary value problem. Also, it is shown in the figure that [P] can be determined at any time (not just at t_0), so that this is equivalent to linear feedback guidance if only this correction is used each time a guidance signal is needed. When this linear correction is combined with the normal procedure for solving the guidance boundary value problem, a type of nonlinear feedback guidance results. More details on this type procedure can be found in Reference 5.

In conclusion it is necessary to reiterate that the improvements made in numerical integration techniques, the improvements in techniques for the solution of simultaneous nonlinear equations, and the expected improvements in guidance computers make optimal guidance appear to be feasible as an onboard guidance scheme and desirable because of its flexibility for different missions and problems. Most of

(1.) λ_0, t_f, ρ, & β ARE DETERMINED FOR A NOMINAL x_0, t_0

(2) THE MATRIX $[P_0]$ IS DETERMINED SUCH THAT

$$\begin{bmatrix} \Delta \lambda_0 \\ \Delta t_f \\ \Delta \rho \\ \Delta \beta \end{bmatrix} = [P_0] \, \Delta x_0$$

THEN AT ANY TIME $t_0 \leq t < t_f$

THE INFORMATION NEEDED TO START THE BOUNDARY VALUE ITERATION IS GIVEN BY NUMERICAL INTEGRATION OF:

$$\begin{cases} \dot{x} = H_\lambda^T \\ \dot{\lambda} = -H_x^T \\ 0 = H_u \end{cases} \quad \text{AND} \quad [\dot{P}] = M\left(t; [P], x, \lambda\right)$$

FIGURE 8. PREFLIGHT CALCULATIONS FOR OPTIMAL GUIDANCE

the derivation and development of the ideas concerned with QUOTA and Optimal Guidance are relatively new, thus there is not a large amount of numerical simulation and documentation available; although some are given in the list of references. Further work is in progress and the results will appear in later publications and presentations.

REFERENCES

1. Ingram, Hugo L.: The Automation of Optimization Problems. Vol. II of the AAS Science and Technology Series, 1967.

2. Burrows, Roger R.; and McDaniel, Gary A.: A Method of Trajectory Analysis with Multi-Mission Capability and Guidance Application. Preprint for the AIAA Guidance, Control, and Flight Dynamics Conference, 1968.

3. Smith, I.E.: General Formulation of the Iterative Guidance Mode. NASA TM X-53414, March 22, 1966.

4. Brown, K. R.; and Johnson, G. W.: Real-Time Optimal Guidance. IGM Report No. 66-220-0001, August 30, 1966.

5. Friedland, Bernard; Welt, Sanford; and Richman, Jack: Guidance Applications of a Quasi-Optimum Control Technique. Final Report for Contract No. NAS8-20311, Nov. 15, 1967.

Page Intentionally Left Blank

RENDEZVOUS TECHNIQUES

By

Wayne Deaton and Wendell Elrod

SUMMARY

This paper presents the overall progress made by the Aero-Astrodynamics Laboratory's Guidance Branch in the area of rendezvous techniques research which encompasses orbital mechanics, trajectory shaping, profile selection, guidance compatibility, and targeting data generation.

INTRODUCTION

This paper describes research work performed on the Apollo Projects and the Apollo Applications Projects. This research work was required to solve the operational problems encountered on a mission to mission basis. The task of achieving rendezvous of two spacecrafts in orbit is an integral part of the mission plans of both the mainstream Apollo Lunar Landing Mission and the Apollo Applications Program Missions. Therefore, it is evident that research in the area of rendezvous techniques plays an important role in the present and future plans of Marshall Space Flight Center and NASA.

Given a rendezvous mission and the characteristics of the launch vehicles to be used in the mission, the methods of achieving rendezvous are divided into essentially four phases of operation. The first phase of rendezvous normally starts with the prelaunch analysis with both vehicles on the ground. After sufficient analysis and planning, the first vehicle is launched into some desired earth parking orbit. The second phase begins while the second (pursuit) vehicle is still on the launch pad. The operational plans have to be established so that lift-off time and targeting conditions can be determined for the second launch vehicle. The third phase begins with the two vehicles in different orbits. Transfer maneuvers have to be determined that will permit position intercept to occur and a velocity matching maneuver to place the two vehicles in a station keeping mode. The fourth phase is the final docking phase and will not be discussed in this paper.

The prelaunch analysis required in planning a rendezvous mission represents a tremendous amount of work; therefore, doing justice to this topic is outside the scope of this paper. A brief discussion of the features of rendezvous mission planning will be presented at the end of this paper. However, since the orbital parameters of the target satellite dictate the performance requirements of the pursuit launch vehicle, it seems worthwhile, and perhaps fundamental, to examine the desirable features of selecting a set of orbital conditions that will be compatible for the second launch and subsequent rendezvous.

RENDEZVOUS COMPATIBILITY

Rendezvous compatibility applies to an orbit that periodically phases with the launch site in such a manner that no plane change will be required in the ascent trajectory to achieve rendezvous. A daily rendezvous compatible target orbit, whose inclination must be equal to or greater than the latitude of the launch site, allows an inplane rendezvous ascent trajectory profile to occur nearly over the launch site either once or twice per day. The only requirement for the one opportunity per day case is that the target satellite appears above the launch site at the same times on successive days. Since the radius of a circular orbit determines its period, the proper choice of altitude alone is sufficient to permit correct phasing. That is, the altitude should be chosen so that the orbital period will divide into 23 hr and 56 min an integer number of times.

The computed orbital period must be corrected to compensate for the oblateness of the earth. The major effect of oblateness on a circular orbit is the precession of the orbital plane whose rotational direction about the polar axis is opposite to the general direction of motion of the satellite. Thus, for an eastwardly traveling satellite, the nodal rate with respect to the earth is the sum of the earth's rotational rate and the nodal precession rate of the orbit.

The basic targeting angles required to specify an earth parking orbit that will require no plane change in an ascent trajectory from a purely spherical earth standpoint is displayed by Figure 1. The launch azimuth measured from true north is shown by the angle A_Z. The geodetic latitude of the launch site is denoted by the angle ϕ_L and the orbital inclination and descending node by the angle i and θ_N, respectively. Those angles will be needed for establishing inplane rendezvous compatible targeting data.

To establish a twice per day rendezvous compatible orbit, separated by one complete orbit, only discrete combinations of inclination and altitude will satisfy the phasing requirements since a relationship between the time for the earth to move a fraction of a revolution and the time for the satellite in orbit to travel the necessary distance must be satisfied. The orbital trace of a twice per day rendezvous compatible target satellite orbit separated by one orbit is illustrated by Figure 2. The circular orbit altitude selected was 185.2 km (100 n. mi.) and the orbital inclination was 28.896 degrees. After 16 orbits, the target satellite will be in proper phase

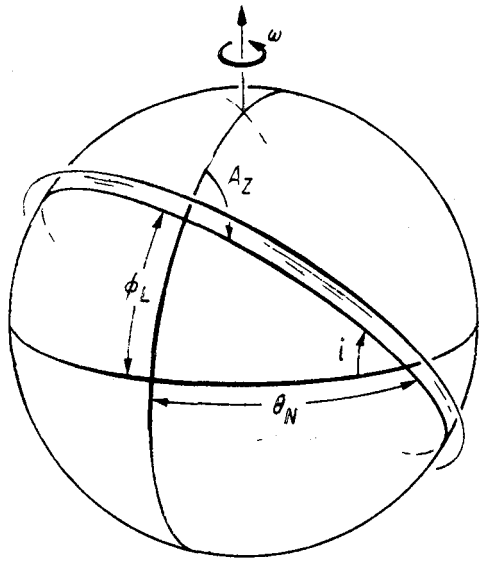

FIGURE 1. DESCRIPTION OF EARTH PARKING ORBIT

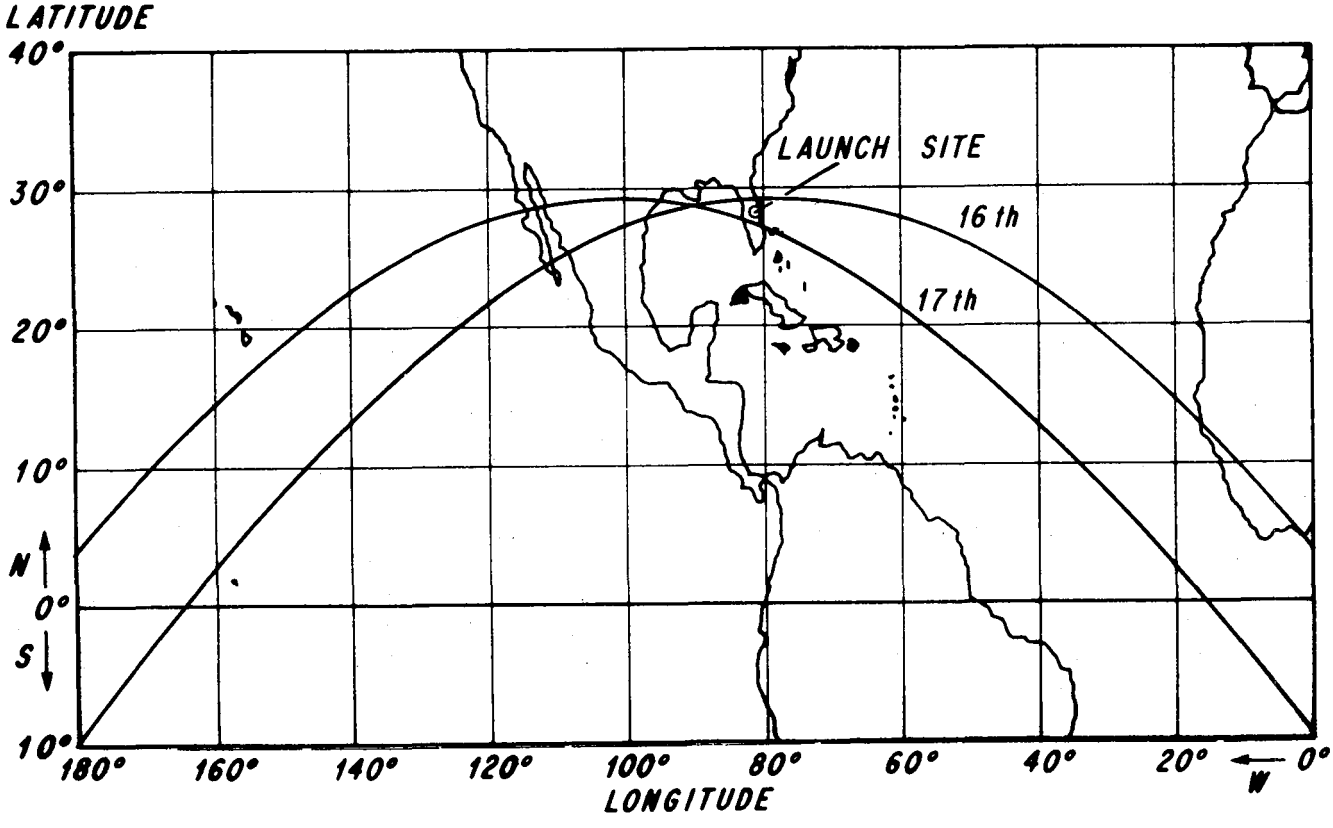

FIGURE 2. ORBITAL TRACE

for a northerly inplane launch and one orbit later (17th orbit) a second inplane launch can be achieved with a southerly launch azimuth. Once the orbital inclination and circular orbit altitude for a rendezvous compatible orbit have been defined, the relationship governing the choice of launch azimuth and the corresponding value of the orbital descending node can be derived from spherical trigonometry (see Fig. 1).

If the launch azimuth is varied from north to south and the corresponding orbital inclination and descending node are determined that satisfy inplane launch parameters, inclination versus descending node becomes a double valued function with the minimum inclination equal to the latitude of the launch site as indicated by Figure 3. It is easy to see from Figure 3 that for the same value of inclination, the separation in descending node must be perfect if an inplane condition is to exist one, two, or three orbits later. P_c in Figure 3 represents the orbital period corrected for the movement of the launch site from one orbit to the next and ω represents the combined effect of the earth's rotational rate and the nodal regression rate as a result of the oblateness of the earth acting on the target satellite.

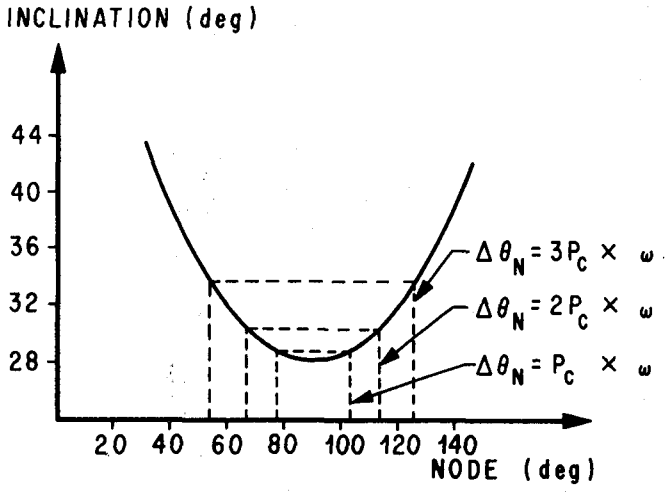

FIGURE 3. INCLINATION VERSUS NODE FOR A COPLANAR LAUNCH

Now that rendezvous compatibility conditions have been analyzed, the next step is to examine the consequences of nonrendezvous compatible target satellite orbits on the pursuit launch vehicle performance. The effect of noncompatibility is simply that when the launch site moves to an inplane condition with the satellite orbit, the satellite's location in orbit is out of phase with the pursuit vehicle at orbital insertion. The mission planner would have essentially three options available: (1) The pursuit vehicle could be launched inplane (biased by the nodal regression rate differences) and accept the phase error and plan to take these errors out by proper selection of the geometry of the orbits. (2) The pursuit vehicle could accept the performance penalty for launching inphase and subsequently make a plane change maneuver to properly align the two orbital planes. (3) The pursuit vehicle could be launched in some compromise between inplane and inphase. Figure 4 illustrates the plane change penalty associated with selecting a target satellite orbit that is rendezvous noncompatible. The phase error will cause a day to day shift in the pursuit vehicle targeting requirements until it is impossible to achieve orbital insertion strictly from a plane change standpoint. The plane change penalties become more severe for the higher target satellite inclination cases.

The importance of prelaunch analysis from the viewpoint of rendezvous compatibility and launch vehicle performance to the mission planners can be illustrated by discussing a particular rendezvous problem. Suppose a space station was in operation at an orbital inclination of approximately 34.3 degrees and a circular orbit of approximately 407 km (220 n. mi.). This particular combination of orbital parameters will yield two launch opportunities separated by three orbits and occurring inphase every five days. Suppose for some reason a critical resupply mission (or rescue) was required just after one of the rendezvous compatible days had been passed. Since the launch site will pass through two inplane launch opportunities per day, the value of having the capability of correcting the phasing errors by proper selection of the geometry so that a sizeable period difference can be realized between the two orbits can be an advantage. If a direct ascent type rendezvous scheme is selected for this type of mission, then it could be that resupply or rescue capability would occur only on rendezvous compatible days.

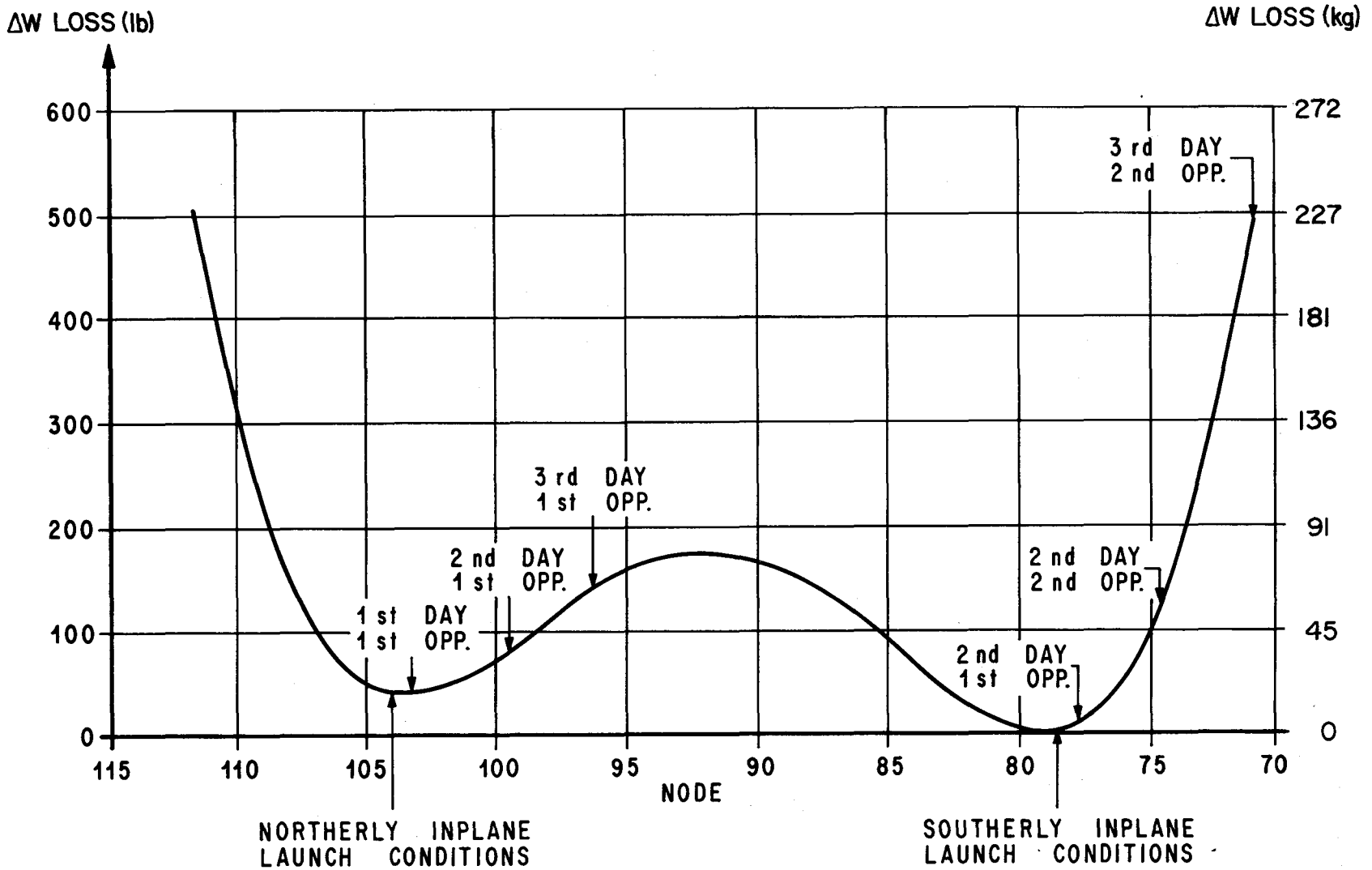

FIGURE 4. RENDEZVOUS NONCOMPATIBLE PENALTY

RENDEZVOUS PROFILES AND LAUNCH WINDOWS

The topics covered thus far have centered around selecting desirable target satellite orbits that tend to simplify the launch operations of the pursuit launch vehicle. The discussion will now shift to that of selecting pursuit vehicle rendezvous profiles that meet all the requirements for rendezvousing with a target satellite in some given orbit. For simplicity, the assumption will be made that the target satellite is in some given circular orbit; although, all profiles discussed will also apply to elliptical target satellite orbits.

The problems of selecting a rendezvous profile can best be described by reviewing some of the profiles analyzed for the proposed Apollo Applications Program Mission (AAP-4). For the planned AAP-4 mission an unmanned Lunar Module minus the descent stage with an attached Apollo Telescope Mount (LM/ATM) will rendezvous with an orbital assembly composed of a spent S-IVB stage workshop (OWS) multiple docking adapter, and a docked command and service module (CSM) with a three man crew on board. The launch vehicle configuration consisted of a S-IB first stage, S-IVB second stage, and the LM/ATM payload which has only the low thrust reaction control system (RCS) for maneuvering and attitude control. There were five profiles selected for analysis from a launch window and vehicle performance standpoint.

The basic co-centric orbit rendezvous approach will be considered first since it was the basic rendezvous plan used in project Gemini and represents essentially the simplest plan from an operations viewpoint of any rendezvous profile. The co-planar profiles and maneuver points are shown in Figure 5 and labeled mode 1. The S-IVB-LM/ATM would be inserted into a circular orbit either below and behind or above and ahead of the OWS. The separated LM/ATM would remain in the lower orbit (below and behind) in a catch-up mode until the phasing was proper to initiate an intercept transfer maneuver and then a velocity correction to match orbits in a station-keeping state. Midcourse corrections would be required to compensate for navigational uncertainties. The phasing orbit can be used to take out launch vehicle insertion dispersions and build a launch window. For a 18.5 km (10 n.mi.) height differential in near earth space, the average orbital rate difference is approximately 0.0006 degrees/sec. At this orbital rate difference, it would require 1,000 sec in the catch-up mode to offset the phasing of a 10-sec launch window. Any variation to this simple plan means complicating the rendezvous maneuvers and increasing the vehicle performance requirements (ΔV, delta velocity).

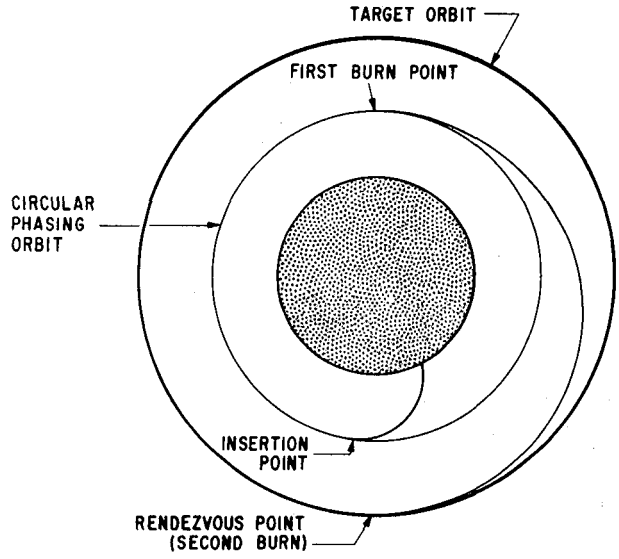

FIGURE 5. MODE 1

Mode 2 illustrated by Figure 6 is a rendezvous scheme that uses elliptical phasing to build a launch window and take out insertion dispersions in the power flight burn arc. The LM/ATM is inserted into an elliptical orbit that intersects the circular target orbit with a fixed perigee radius. Obviously, either intersection point could be selected as an orbital transfer point, but not both, since the two points represent different phase relationships. The target orbit shown here could be a position rendezvous point or some desirable transfer orbit whereby a series of maneuvers could be made to enhance a position rendezvous at a low closing rate. The correct phasing between the orbital workshop and the LM/ATM is determined by selecting the proper apogee height to enforce the transfer or intersection point. The limit to the amount of launch window that can be built with this mode is determined by the geometry limit (target and LM/ATM orbit tangent), the launch vehicle performance limit, and the number of phasing orbits allowed. Since the Saturn launch vehicle guidance system predicts the range angle and flight time to orbital insertion, it is a simple operation to determine the phasing error for an inflight performance perturbation and correct the apogee height to restore

correct phasing. This technique of power flight phase correction will be covered in greater detail later in the paper.

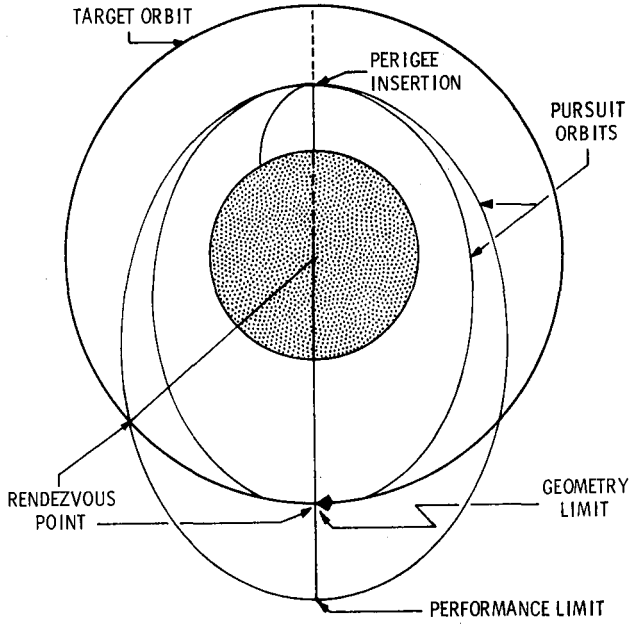

FIGURE 6. MODE 2

Another mode of operation for achieving rendezvous is possible by inserting the LM/ATM into a fixed ellipse defined by a selected perigee radius below the target circular orbit radius. After LM/ATM coast to apogee, a maneuver would be initiated to adjust the perigee radius to correct the phasing error and build a launch window. A second maneuver would then be initiated at second apogee passage to match the OWS orbit and achieve a station-keeping state. The amount of launch window available is, of course, limited by the perigee variation possible and the number of phasing orbits permitted before the second maneuver. The amount of phasing possible is directly controlled by the orbital period difference between the target and pursuit orbits. This mode is illustrated by Figure 7 and known as mode 3. A variation to this method would be a direct insertion into the OWS orbit and maneuver to raise apogee to correct any phasing errors and a subsequent second maneuver at perigee to match orbits at a station-keeping distance.

Since a launch window can be built by both perigee and apogee radius variations, mode 4 (Fig. 8) considers the basic features of such a mode of operation to achieve rendezvous. This method of

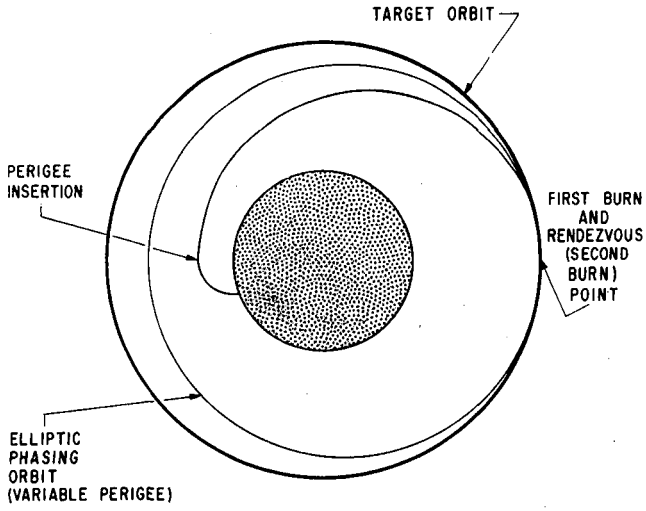

FIGURE 7. MODE 3

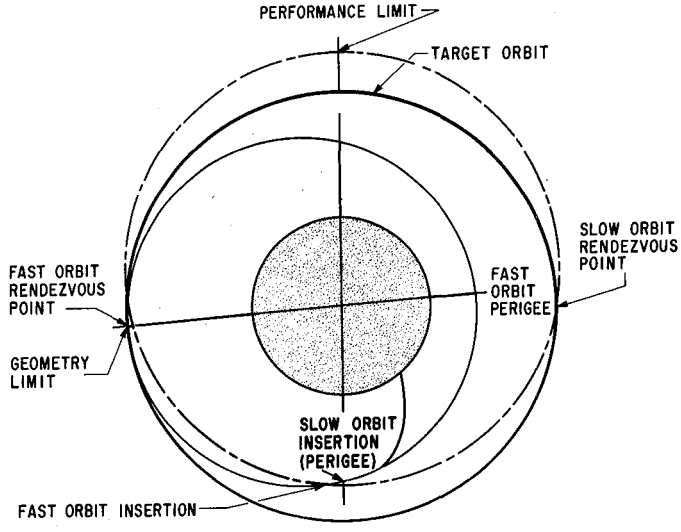

FIGURE 8. MODE 4

obtaining a rendezvous combines the features of mode 2 and mode 3. Since the Saturn IB S-IB stage uses an open-loop time-dependent steering program, this steering program should be selected for the worse performance case, which would be a high perigee radius and a maximum apogee radius that will still satisfy the mission performance requirements. This trajectory profile will represent the slowest of the LM/ATM orbits (largest orbital period) that would permit a position intercept. As the phasing requirement changes across the launch window, the perigee altitude would be lowered to speed up the LM/ATM orbital rate (shorten the orbital period). This procedure would conflict with

the open-loop steering program since it was designed for a high perigee insertion. Since the open-loop steering program is a strong function of the altitude of orbital insertion, the difficulty can be overcome by rotating the perigee radius (line of apsides) until the altitude of orbital insertion is nearly equal to the slow orbit perigee insertion altitude. The apogee radius is then determined to satisfy the required phasing and hence rendezvous. The perigee radius is continually lowered until the minimum allowable altitude is reached, 150 km (81 n. mi.), and the geometry limit is reached (LM/ATM apogee radius tangent to the OWS orbit). At LM/ATM lift-off, the location of the perigee radius and its magnitude is determined as well as the corresponding apogee radius magnitude to insure correct phasing. During power flight, the apogee radius magnitude will be permitted to vary to take out down range insertion dispersions the same as mode 2. This mode combines the best features of each scheme to yield the maximum launch window; but, it represents the most difficult one to implement because of the additional targeting requirements.

The next mode of operation to be considered uses essentially a fixed ellipse; but allows rotation of the line of apsides to correct phasing errors. The coplanar geometry of mode 5 is displayed by Figure 9. The LM/ATM orbit has a fixed perigee radius and an apogee radius that is equal to the circular target orbit at the tangency point (intercept point of the OWS orbit if elliptical). The proper phasing is achieved by rotation of the perigee radius in the LM/ATM orbital plane about the insertion radius. At the opening of the launch window, the LM/ATM would be inserted on a true anomaly greater than zero and achieve an intercept in less than half an orbit. At the middle of the launch window, the LM/ATM would be inserted at perigee and achieve an intercept in exactly one-half an orbit (Hohmann Transfer). At the closing of the launch window, the LM/ATM would be inserted on a negative true anomaly and achieve an intercept between one-half and a whole orbital period. The open-loop steering program would be designed for either the opening or closing of the launch window and does not present a major problem since the performance penalty is decreased with altitude of insertion. If a performance variation were encountered during power flight, the true anomaly can be determined that will enforce the proper phasing. If the OWS orbit were elliptical, the height of apogee would have to become a function of LM/ATM insertion true anomaly so that intercept (or transfer condition) would slide along the surface of the OWS orbit. The advantage to this scheme would be the near constant delta velocity required at the intercept point.

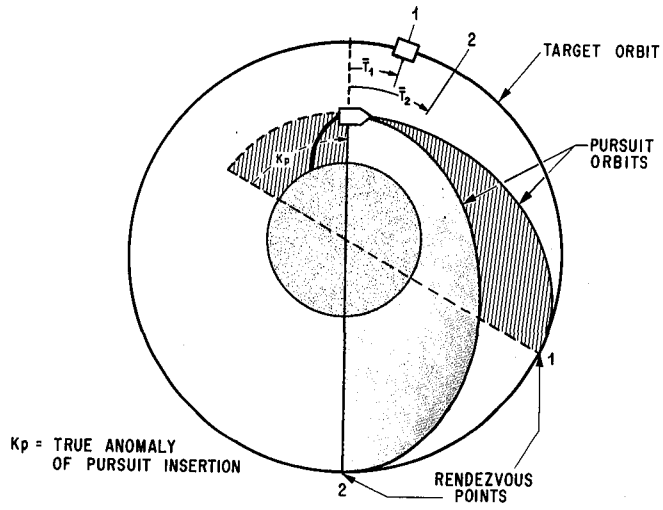

FIGURE 9. MODE 5, RENDEZVOUS VIA ROTATION OF PERIGEE

Since the five modes have been described from a flight and orbital mechanics aspect, the modes will now be summarized using the AAP-4 mission launch vehicle characteristics. The modes will be compared by selection of an arbitrary delta velocity of 75 m/sec for the LM/ATM maneuver at the position intercept point. The OWS orbit is assumed to occupy a 407 km (220 n. mi.) circular orbit. The pertinent data pertaining to the five modes are shown by Table I and will be described in the following paragraphs.

MODE 1

Mode 1, or the co-centric orbit mode, would need to be launched directly into an orbit of 282 × 282 km (152 × 152 n. mi.) so that the combined delta velocity (ΔV) would be 75 m/sec for the two impulse transfers into a 407 × 407 km (220 × 220 n. mi.) orbit. The surplus payload above the required LM/ATM payload for this profile is 2040 kg (4500 lb). The phasing available for 1.5 orbits is 4 min and each additional phasing orbit gives an additional 2.6 min. One and one-half orbits was selected to make the data consistent with mode 2, which assumes one complete orbit and a planned intercept between one orbit and one-half orbit (geometry limit).

TABLE I(A). SUMMARY CHART

MODE		INITIAL ORBITS (FAST) (SLOW)	TRANSFER ORBIT (FAST) (SLOW)	Δ_v	Δ_{wp}	PHASING		NUMBER OF LM BURNS
						AFTER 1.5 ORBITS	EACH ADD. ORBIT	
		km	km	(m/s)	Mg	(min)	(min)	
1 COCENTRIC CIRCLES		282 × 282	282 × 282	75	2.0	4	2.6	2
2 ELLIPTICAL PHASING	S-IVB KICK	148 × 407 148 × 570		250	0	3.5	2.4	0
APOGEE	LM KICK	268 × 407 268 × 443		75	1.8	.7	.5	1
VARIATION	LM KICK	370 × 407 370 × 496		75	0	2.2	1.5	
3 PERIGEE VARIATION		148 × 407	148 × 407 407 × 407	75	3.6	2.6	2.6	2
4 APOGEE & PERIGEE		148 × 407 268 × 443		75	1.8	3.5	2.4	1
VARIATION		148 × 407 370 × 496		75	0	7.5	5	1
5 PERIGEE ROTATION		148 × 407		75	2.7	< 1 ORBIT 2.0	< 2 ORBITS 2.0	1
		204 × 407		60	2.7	< 1 ORBIT 1.2	< 2 ORBITS 1.2	
		259 × 407		44	1.8	< 1 ORBIT 1.0	< 2 ORBITS 1.0	

TABLE I(B). SUMMARY CHART

MODE		INITIAL ORBITS (FAST) (SLOW)	TRANSFER ORBIT (FAST) (SLOW)	Δ_v	Δ_{wp}	PHASING		NUMBER OF LM BURNS
						AFTER 1.5 ORBITS	EACH ADD. ORBIT	
		(n mi)	(n mi)	(m/s)	(klb)	(min)	(min)	
1 COCENTRIC CIRCLES		152 × 152	152 × 152	75	4.5	4	2.6	2
2 ELLIPTICAL PHASING	S-IVB KICK	80 × 220 80 × 308		250	0	3.5	2.4	0
APOGEE	LM KICK	145 × 220 145 × 239		75	4	.7	.5	1
VARIATION	LM KICK	200 × 220 200 × 268		75	0	2.2	1.5	
3 PERIGEE VARIATION		80 × 220	80 × 220 220 × 220	75	8	2.6	2.6	2
4 APOGEE & PERIGEE		80 × 220 145 × 239		75	4	3.5	2.4	1
VARIATION		80 × 220 200 × 268		75	0	7.5	5	1
5 PERIGEE ROTATION		80 × 220		75	6	< 1 ORBIT 2.0	< 2 ORBITS 2.0	1
		110 × 220		60	6	< 1 ORBIT 1.2	< 2 ORBITS 1.2	
		140 × 220		44	4	< 1 ORBIT 1.0	< 2 ORBITS 1.0	

MODE 2

The elliptical phasing by apogee variation approach to rendezvous known as mode 2 has data listed for three cases. Since a low perigee altitude insertion gives such a large payload surplus, it would be possible to use the S-IVB stage in a reignition mode. For the geometry shown for this mode, a total of 3630 kg (8000 lb) above the required LM/ATM payload was reserved for the reignition of the S-IVB stage (2720 kg or 6000 lb for reignition propellants and 910 kg or 2000 lb for additional pressure bottles and ullage rockets). The performance limit for this case is defined by the 148 × 386 km (80 × 208 n. mi.) orbit which is the maximum apogee height possible and still have the 3630 kg (8000 lb) surplus needed for reignition. The delta velocity available for the 2720 kg (6000 lb) of reignition propellants is approximately 360 m/sec. The geometry limit is a 148 × 407 km (80 × 220 n. mi.) ellipse. The transfer delta velocity required to transfer from the 148 × 570 km (80 × 308 n. mi.) orbit to the 407 × 407 km (220 × 220 n. mi.) OWS orbit is 250 m/sec giving a phasing capability of 3.5 min and an additional 2.4 min for each additional phasing orbit. Case 2 gives the geometry range that corresponds to a payload surplus of 1815 kg (4000 lb) and a ΔV or 75 m/sec. Case 3 gives the geometry range for a zero payload surplus giving a phasing time possible of 2.2 min and 1.5 min for each additional orbit as compared to 0.7 and 0.5 min for case 2.

MODE 3

The LM/ATM is inserted into a 148 × 407 km (80 × 220 n. mi.) orbit and the perigee altitude at first apogee passage is varied by the range of 148 to 407 km (80 to 220 n. mi.) to generate a phasing capability of 2.6 min with a surplus payload of 3630 kg (8000 lb). Each additional phasing orbit adds 2.6 min phasing capability.

MODE 4

The apogee and perigee combination yields a 3.5 min launch window for a profile selected to give a 1815 kg (4000 lb) payload surplus and a 7.5 min launch window for a zero payload surplus with each having a 75 m/sec ΔV requirement.

MODE 5

If a 148 × 407 km (80 × 220 n. mi.) phasing ellipse is selected and the true anomaly restricted such that 2720 kg (6000 lb) of payload surplus is conserved, the perigee rotation mode will permit 2.0 min of phasing with a constant ΔV requirement of 75 m/sec. Data are also presented for perigee altitudes of 204 and 259 km (110 and 140 n. mi.).

The trends indicated for these five rendezvous modes will change as the target satellite orbit is raised or lowered since the orbital period difference determines the phasing capability of any rendezvous mode. Again, the AAP-4 mission data were selected only to give some basis for comparison of the five modes.

S-IVB-LM/ATM UNMANNED RENDEZVOUS

The original plans for the AAP-3 and AAP-4 missions called for the AAP-3 launch configurations (S-IB stage, S-IVB and CSM) to be launched into a 220 km (120 n. mi.) circular orbit essentially coplanar with the OWS. On the following day, the AAP-4 launch configuration would insert the LM/ATM into a 296 km (160 n. mi.) circular orbit. The CSM would then use the co-centric rendezvous mode and dock with the LM/ATM. The CSM-LM/ATM would then rendezvous with the orbital workshop. This procedure of dual rendezvous caused several difficulties in terms of vehicle performance and nodal regression when the LM/ATM failed to meet the narrow launch window time resulting in launch delays and crew operation complexities. To solve these problems, NASA Headquarters directed the Manned Spacecraft Center to study the problem from a LM/ATM unmanned rendezvous standpoint and Marshall Space Flight Center to study it using the S-IVB stage to achieve unmanned rendezvous, and deliver the LM/ATM in a station-keeping position at approximately 150 m (500 ft) from the OWS, MDA, and CSM cluster. A discussion of the analysis required to establish feasibility of the S-IVB-LM/ATM unmanned rendezvous should be helpful in understanding the operational problems associated with making modes 2, 3, 4, and 5 successful on a rendezvous mission. The analysis was based on an assumed circular orbit of 407 km (220 n. mi.) for the OWS/MDA/CSM configuration and using mode 2 for achieving rendezvous.

The performance and the launch window characteristics for one complete phasing orbit (N=1) of the S-IVB-LM/ATM before the transfer into an orbit that is co-centric with the orbit workshop configuration is given in Figure 10. Figure 10 indicates the relationship between launch vehicle performance,

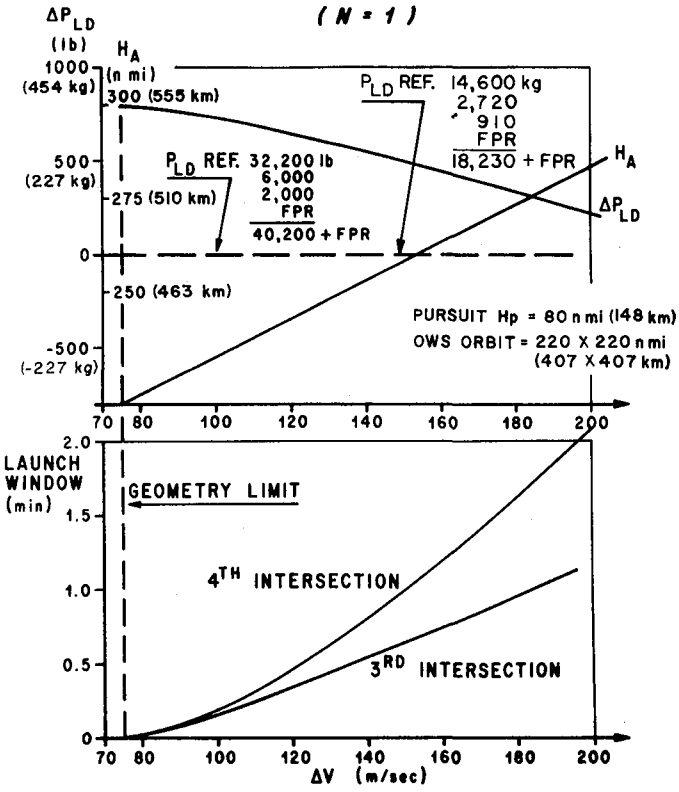

FIGURE 10. MODE 2 PERFORMANCE AND LAUNCH WINDOW CHARACTERISTICS

geometry, transfer impulse (ΔV), and launch window duration. The payload reference ($P_{LD}REF$) for the LM/ATM is 14600 kg (32,200 lb). There were 2720 kg (6000 lb) pounds of propellant, 910 kg (2000 lb) of reignition structure, and the flight performance reserves (FPR) set aside above the reference payload. Delta payload (ΔP_{LD}), height of apogee (H_A), and launch window duration are plotted against the delta velocity (ΔV) required to transfer into the co-centric orbit. The height of perigee of the S-IVB-LM/ATM was selected at 148 km (80 n.mi.) for performance and phase capability. The geometry limit, shown by the vertical dashed line, is a 148 × 407 km (80× 220 n. mi.) Hohmann transfer ellipse. The launch window duration is displayed for using the third intersection (first intersection after one full orbit) and the fourth intersection. A 30-sec launch window and the fourth intersection point, altered to yield a set of transfer conditions 9.26 km (5.0 mi.) below and 0.85 degrees behind the OWS, was used in the feasibility analysis. The orbital transfer maneuver was performed by using the S-IVB stage in a reignition mode of the main propulsion system (J-2 engine). The orbital trim, plane change, and rendezvous transfer maneuvers used a modified S-IVB stage auxiliary propulsion system with longitudinal thruster capability.

The task of making any rendezvous mode successful in a real mission depends upon how accurately and how rapidly the launch vehicle targeting data can be determined based upon the target orbital ephemeris. Keplerian solutions can be used to generate the targeting data if detailed orbital tracking and orbital corrections are included in the mission plan; but, this can become expensive in terms of propellant comsumption. The orbital perturbation effects of atmospheric drag, propulsion venting, and the oblateness terms of the gravity model make corrections to the Keplerian solutions to targeting data a necessity regardless of what mode of operations is selected to achieve rendezvous. A flow chart in block diagram form for determining the refined launch vehicle targeting data for the pursuit launch vehicle is illustrated by Figure 11. The target satellite ephemeris data are used in a block of Keplerian equations in which solutions are obtained as initial targeting estimates to a more complex numerical model. This numerical model will determine the necessary corrections to the pursuit orbital plane and conic energy needed to generate the rendezvous solution (or transfer conditions) for any particular mode selected under the orbital perturbations of atmospheric forces, propulsion venting, and the non-uniformity of the gravitational field. These numerical solutions are then processed through a launch vehicle targeting function generator to obtain targeting data in a form that can be implemented in the launch vehicle digital guidance computer. This particular method of generating launch vehicle targeting data can be accomplished in less than 15 minutes with the present high speed digital computers, making it a feasible system from an operational standpoint.

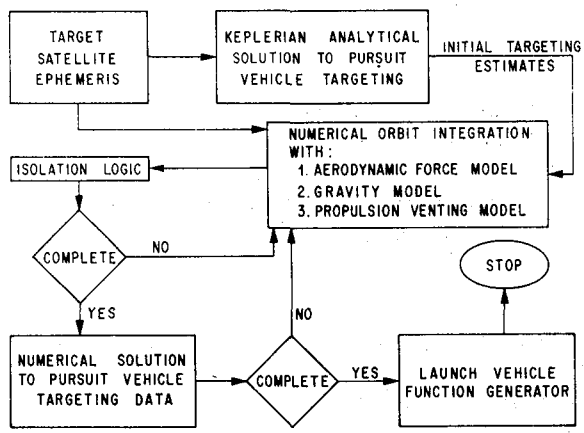

FIGURE 11. TARGETING DATA FLOW CHART

Since the method of generating targeting data has been discussed, it seems noteworthy to cover the required modifications to the present Saturn IB guidance equations (iterative guidance mode - IGM) to implement a rendezvous scheme that can be used to build a launch window and restore correct phasing during power flight to compensate for any power flight performance perturbations. The details of the guidance system will not be discussed since adequate documentation is given in the references. The basic block diagram form of the guidance equations, shown in Figure 12 illustrates the modifications required to implement any of the rendezvous modes that permit phase correction during power flight (modes 2, 4 and 5). The inputs to the guidance computer are: I. Vehicle parameters (mass, mass rate, burning time of each stage, and specific impulse); II. Target parameters (radius of perigee, radius of apogee function, orbital plane regression function, and launch window duration); III. Guidance options (fixed end conditions, variable end conditions, range angle update, and terminal coordinate system rotation). The precomputation section of the ascent guidance system uses the lift-off signal to set the desired orbital plane orientation (inclination and descending node), define the conic parameters, and orient the major axis of the conic. Normally the guidance equations will use the current navigational information of the vehicle state to determine the range angle and flight time to orbital insertion (Fig. 12, 1 and 2) and then evaluate the remaining closed integrals so that steering commands (Fig. 12, 6 and 7) can be issued to the control system network, and thereby, enforce a desired set of terminal conditions. The software (equation changes) required to implement modes 2, 4, and 5 are shown as statement number 3, 4, and 5 in Figure 12 under the heading guidance equations. The predicted range angle and time of flight

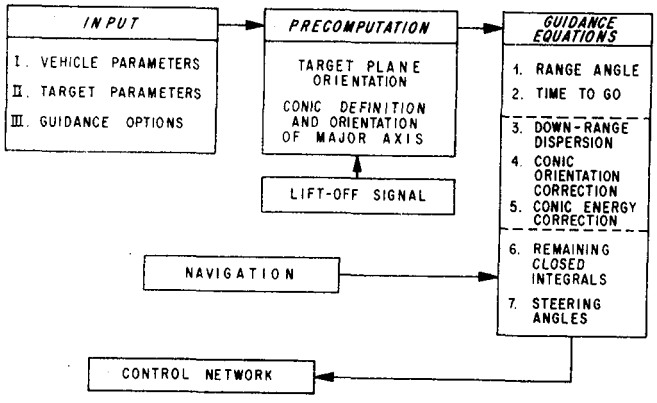

FIGURE 12. ASCENT GUIDANCE FLOW CHART

to orbital insertion can be used to determine the down range dispersion of this insertion point, and hence, the phase error between the target and pursuit vehicles. The phase error can then be used to determine the corresponding conic orientation and energy correction needed to restore proper phasing at orbital insertion so that rendezvous can occur in an economical fashion with respect to time and vehicle propellant budgets.

The co-planar geometry of one particular method of using mode 2 to achieve a station keeping position between the S-IVB-LM/ATM and the orbital assembly is illustrated by Figure 13. The geometry is shown for achieving rendezvous by transferring into an orbit below and behind the OWS and then an intercept transfer maneuver to place the S-IVB-LM/ATM on an intercept course with the OWS. The S-IVB-LM/ATM would then perform a velocity matching maneuver at the station-keeping position. The targeting can just as easily be determined for transferring above and ahead of the OWS or a direct insertion into the workshop orbit by some given lead or lag angle. A series of transfer maneuvers could then be used to achieve rendezvous.

The uncertainties of the navigation information available to the S-IVB-LM/ATM make orbital trim maneuvers a necessary part of achieving rendezvous. After performing the orbital transfer maneuver into a set of conditions below and behind the orbital workshop, the Lunar Module rendezvous radar data and advance OWS ephemeris data can be used to correct the orbital elements of the S-IVB-LM/ATM. The inplane corrections would be performed at maneuver 3 (height adjustment) and the out-of-plane corrections would be applied at the line of nodes between the OWS orbit and the S-IVB-LM/ATM orbit denoted by maneuver 4. Maneuver 4 would always occur within one-half an orbit after maneuver 3. After sufficient time in the lower catchup orbit to allow proper phasing to occur, the terminal rendezvous transfer maneuver would be initiated (maneuver 4) and a subsequent final velocity matching maneuver at position 6. Midcourse corrections between maneuvers 5 and 6 can be applied to reduce the errors caused by radar measurement noise.

The guidance equations (software) required to perform the orbital trim maneuvers and the rendezvous transfer maneuvers are presently under development. The ΔV requirements for these maneuvers are normally small and velocity steering is adequate without any appreciable vehicle performance losses. The feasibility analysis of using the S-IVB stage

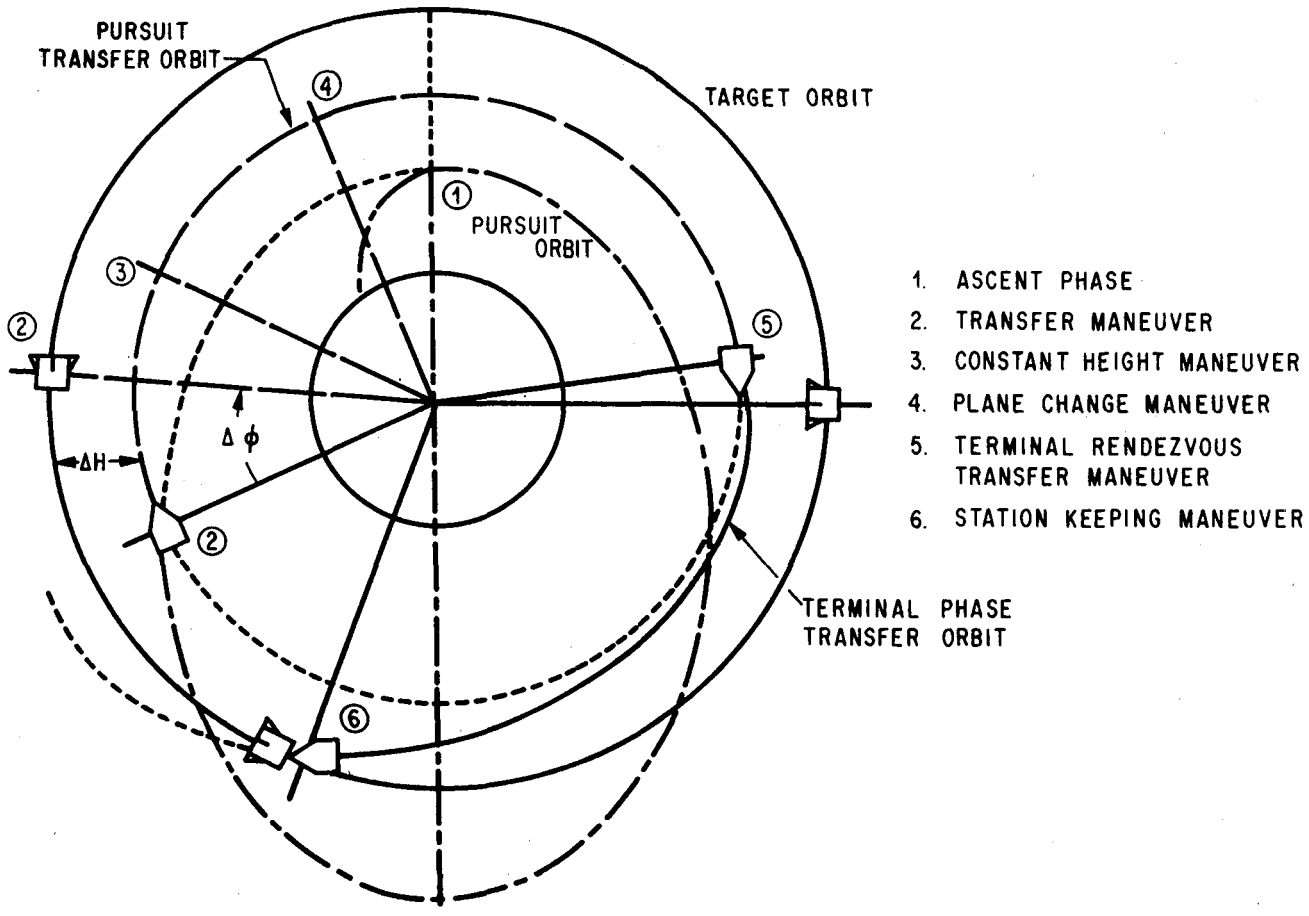

FIGURE 13. MODE 2 RENDEZVOUS MANEUVERS

in a reignition mode and using the modified auxiliary propulsion for the orbital trim and rendezvous transfer maneuvers indicate that the S-IVB-LM/ATM is feasible from the standpoint of performance, guidance, and system lifetime in orbit. The results of a detailed analysis will be documented at a later date. The use of the S-IVB stage to rendezvous orbital workshops and resupply modules in high circular or elliptical orbits has been verified by this feasibility analysis. For circular orbits much above 370 km (200 n. mi.) the high thrust of the S-IVB J-2 engine becomes incompatible with the altitude constraint, and it becomes more economical to use a thrust-coast-thrust trajectory profile. The useful payload can be improved over the bulky adapted lunar module payload by more effective use of the S-IVB stage and a redesign of the S-IVB payload package. Modifications in the propulsion system of the J-2 engine may make reignition available in the near future with lower propellant levels, thus increasing the payload capability of the S-IVB stage.

RENDEZVOUS MISSION PLANNING

A detailed discussion of the essential features of rendezvous mission planning is outside the scope of this paper and only a few words about the major items will be included to indicate its importance to mission success. The items to be discussed are given in Table II.

The launch vehicle performance capability will dictate the range of geometry available for rendezvous flight profile selection. This could very easily determine whether mode 1, 2, 3, 4, 5, or some other mode would be selected to accomplish rendezvous phasing.

A combination of launch probability and urgency of launch will establish the required time duration of a launch window. If there were no urgency of launch considerations and a 50-50 chance of achieving

a count-down to a launch on time, then a selection of a launch window of zero would be justified. If a hold occurred during countdown to zero, the launch vehicle would simply be prepared for the next launch opportunity. If there were a high priority given to achieving a launch vehicle lift-off (critical resupply, rescue, etc.) then a launch window within the performance capability of the launch vehicle would be a desirable feature.

The success of any rendezvous mission is strongly influenced by the orbital tracking capability of the target satellite since this will establish the orbital ephemeris from which targeting data must be derived for the pursuit launch vehicle. The orbital trim maneuvers will be smaller as the uncertainties in the target ephemeris are reduced.

The terminal rendezvous hardware (optical or radar tracking) and the flight crew training (manned flight) will also have an influence on the geometry selected to achieve rendezvous.

The launch vehicle guidance system capability and flexibility will also influence the freedom of selection of geometry to be used in the rendezvous mission. As the flexibility of the guidance system is increased, more and more flight geometry profiles are available to the mission planners.

If the target satellite has an active propulsion capability, then trade-offs between the target and pursuit vehicle propulsion budget are possible. An example of this can be found in the mainstream Apollo lunar landing mission in which the lunar module will rendezvous with the command and service module after descending to the lunar surface and completing the required experiments. The CSM will perform orbital trim maneuvers to keep the LM rendezvous ascent geometry planar. The CSM can also perform limited LM rescue maneuvers if the LM fails to achieve rendezvous.

Mission objectives and many other factors influence the selection of flight profiles and modes of operation to be used in performing a rendezvous mission.

TABLE II. FEATURES OF RENDEZVOUS MISSION PLANNING

1.	LAUNCH VEHICLE PERFORMANCE CAPABILITY
2.	LAUNCH PROBABILITY
3.	SYSTEMS LIFETIME IN ORBIT
4.	ORBITAL TRACKING CAPABILITY
5.	TERMINAL RENDEZVOUS HARDWARE (OPTICAL OR RADAR)
6.	FLIGHT CREW TRAINING
7.	LAUNCH VEHICLE GUIDANCE SYSTEM CAPABILITY AND FLEXIBILITY
8.	TARGET SATELLITE CAPABILITY (PASSIVE OR ACTIVE)
9.	MISSION OBJECTIVES AND OTHER CONSIDERATIONS

CONCLUSIONS

This paper discussed the overall progress made by the Aero-Astrodynamics Laboratory's Guidance Branch in the area of rendezvous techniques, which encompass orbital mechanics, trajectory shaping, profile selection, guidance compatibility, and the generation of targeting data. Hopefully, the reader will become more aware of the factors that have to be considered before selecting a final flight plan for any particular rendezvous mission. The data presented on the AAP-4 mission are to be treated as preliminary and used only as a means of comparison for the different flight profiles considered to achieve rendezvous.

BIBLIOGRAPHY

1. The Boeing Company (Guidance and Navigation Unit): Saturn V Launch Vehicle Guidance and Navigation Equations, SA-504. Report D5-15429-4A, The Boeing Company, September, 1966.

2. Karacsony, P. J.; Petty, R. L.; Sichi, F. J.; and Woodruff, P. G.: Apollo Mission AS-207/208A Preliminary Spacecraft Reference Trajectory. 3902-H015-R0-000, TRW Note No. 66 FMT-412.

3. Kenehan, M. F.: Mission Analysis of Gemini/Agena Rendezvous with Assigned Targets. 3150-6015-R0000, TRW Systems.

4. Petersen, N. V.; and Swanson, R. S.: Rendezvous Compatible Orbits. Astronautical Sciences Review, October - December 1959.

5. Smith, I. E.; and Cooper, F. D.: Launch Vehicle Guidance Equations for the Saturn IB SA-202 Mission. NASA TM X-53266, May 1965.

6. Smith, I. E.: General Formulation of the Iterative Guidance Mode. NASA TM X-53414, March 1966.

7. Swanson, R. S.; and Petersen, N. V.: The Influence of Launch Conditions on the Friendly Rendezvous of Astrovehicles. Proceedings of the AAS-Second Western National Meeting, Los Angeles, California, August 1959.

APPROVAL

RESEARCH ACHIEVEMENTS REVIEW
VOLUME III REPORT NO. 2

The information in these reports has been reviewed for security classification. Review of any information concerning Department of Defense or Atomic Energy Commission programs has been made by the MSFC Security Classification Officer. These reports, in their entirety, have been determined to be unclassifed.

These reports have also been reviewed and approved for technical accuracy.

E. D. Geissler

E. D. GEISSLER
Director, Aero-Astrodynamics Laboratory

UNITS OF MEASURE

In a prepared statement presented on August 5, 1965, to the U. S. House of Representatives Science and Astronautics Committee (chaired by George P. Miller of California), the position of the National Aeronautics and Space Administration on Units of Measure was stated by Dr. Alfred J. Eggers, Deputy Associate Administrator, Office of Advanced Research and Technology:

"In January of this year NASA directed that the international system of units should be considered the preferred system of units, and should be employed by the research centers as the primary system in all reports and publications of a technical nature, except where such use would reduce the usefulness of the report to the primary recipients. During the conversion period the use of customary units in parentheses following the SI units is permissible, but the parenthetical usage of conventional units will be discontinued as soon as it is judged that the normal users of the reports would not be particularly inconvenienced by the exclusive use of SI units."

The International System of Units (SI Units) has been adopted by the U. S. National Bureau of Standards (see NBS Technical News Bulletin, Vol. 48, No. 4, April 1964).

The International System of Units is defined in NASA SP-7012, "The International System of Units, Physical Constants, and Conversion Factors," which is available from the U. S. Government Printing Office, Washington, D. C. 20402.

SI Units are used preferentially in this series of research reports in accordance with NASA policy and following the practice of the National Bureau of Standards.